Contribution to the Geomechanical Stability Analysis of a Marble Underground Exploitation using Rockfill

Mariel Formoso Franqueira

Thesis to obtain the Master of Science Degree in

Master Degree in Mining and Geological Engineering

Supervisor: Professor Gustavo André Paneiro

Examination Comittee

Chairperson: Prof. Maria Amélia Alves Rangel Dionísio

Supervisor: Prof. Gustavo André Paneiro

Members of the Committee: Prof. Maria Matilde Mourão de Oliveira Carvalho Horta Costa e Silva

July 2020

Declaration

I Mariel Formoso Franqueira, student at Instituto Superior Técnico nº ist194925, author of the dissertation to obtain the Master's Degree in Engineering of Mining and Geological Engineering, with the title "*Contribution to the Gomechanical Stability Analysis of a Marble Underground Exploitation using Rockfill*" I grant Instituto Superior Técnico a perpetual, but not exclusive, license to use this dissertation for the purposes of teaching or research and I authorize to insert it, as well as its extended summary, in pdf format, on your website, with address www.tecnico.ulisboa.pt in order to allow its dissemination to all who access that page, and, with the same purpose of dissemination, to respond favorably to requests from educational or research institutions and Documentation Centers or Libraries, sending them those same files in pdf format, but making an express mention, either in su the page on the internet is when the aforementioned referral is made, the obligation of whoever accesses that my dissertation and its respective extended summary to safeguard my copyright on these documents, which are conferred on me by the Copyright and Related Rights Code.

Lisbon, 26 of July of 2020

I declare that this document is an original work of my own authorship and that it fulfills all the requirements of the Code of Conduct and Good Practices of the Universidade de Lisboa.

Abstract

The present work carries out a stability analysis for a Portuguese marble quarry, in prospects of initiating a new underground excavation by means of the room and pillar method. Given the data provided by laboratory and in situ tests as well as a thoroughly geology acknowledgment of the area, so called, Estremoz anticline, and starting from a simplified model of the current open pit, a new excavation design was presented for the underground phase the quarry has started to transition. In order to elaborate, model and estimate the behavior of such excavation in three dimensions, the Finite Element Method software, RS3 from Rocscience, was used. Besides from studying global and local stability in the openings, an idea of contributing to circular economy and environmental sustainability was introduce by making an use of the quarry's waste rock, as the principal aggregate for a backfill material that not only reduces the impact of wastelands in the surface but also acts as support for the newly excavated area and a mean to recover the residual pillars.

Key words

Finite Element Method, Rockfill, Underground quarrying, Stability analysis, Circular economy, Marble

Resumo

O presente trabalho realiza uma análise de estabilidade para uma pedreira de mármore portuguesa, em perspectiva de iniciar uma nova escavação subterrânea por meio do método das câmaras e pilares. Dados os dados fornecidos por testes laboratoriais e in situ, bem como um profundo reconhecimento geológico da área, o chamado anticlíneo de Estremoz, e partindo de um modelo simplificado do actual fosso aberto, foi apresentado um novo desenho de escavação para a fase subterrânea, a pedreira começou a transitar. A fim de elaborar, modelar e estimar o comportamento de tal escavação em três dimensões, foi utilizado o software com o Método dos Elementos Finitos, RS3 da Rocscience. Além de estudar a estabilidade global e local nas aberturas, foi introduzida uma ideia de contribuir para a economia circular e a sustentabilidade ambiental, fazendo uso dos rejeitos da pedreira, como principal agregado para um material de aterro que não só reduz o impacto das terras residuais na superfície, mas também actua como suporte da área recentemente escavada e como meio de recuperação dos pilares residuais.

Palavras chave

Método dos elementos finitos, Rockfill, Pedreiras subterrâneas, Análise de estabilidade, Economia circular, Mármore

Acknowledgements

First of all, I would like to thank Ezequiel Francisco Alves Lda., in the persons of Mr. António Alves and Mrs. Maria Ana Alves for the opportunity to use all data that allowed me to develop my master thesis. With this dissertation I acquired broad knowledge about underground excavation stability in ornamental stone quarries and also other transversal abilities that would be important for my future.

I would like also to acknowledge Instituto Superior Técnico of Universidade de Lisboa, especially, to my supervisor, Professor Gustavo Paneiro for his unconditional support and also my fellow colleague Bernardo Candeias for his support throughout the numerical modelling.

To my parents that fought for my future. Without them this would not be possible.

To the Technical University of Madrid and my supervisor there, Professor José Miguel Galera Fernández.

At last, to my friends who are a big support. Thank you.

Contents

List of Figures

List of Tables

1. Introduction

1.1. Motivation and Objective

The production of ornamental stones takes on noticeable importance in the sector of natural building materials, both from economic and technological point of view. The exploitation of ornamental stone in Portugal consists essentially of marbles, limestones, shales and granites, which are commercialized in three different types of products: blocks that are extracted directly from the quarries; sawn or polished slabs; and the final finished product that results from the cutting of slabs submitted to secondary cutting, surface finishing, selection and packaging. A fundamental factor in the ornamental stone industry is the commercial value of the outcropping rock material, which is the result of a set of parameters, intrinsic and extrinsic to the raw material, of complex determination, and related to its possibilities of extraction, processing, use and marketing. Quarrying in Portugal is an industrial activity with strong traditional roots and with a big impact on national Gross Domestic Product, and its exploitation is of high importance. In the image below, Figure 1, it shows different types of ornamental stones that are exploited all over the country.

Figure 1. Distribution of Portugal's ornamental stone deposits. (Carvalho et al., 2008).

Portugal's marble also counts with an almost uninterrupted exploitation since the times of occupation of the Iberian Peninsula by the Roman Empire that has provided to this time with world reputation and benefits (Carvalho et al., 2013).

In spite of its high profitability, marble is a non-renewable geological resource, humans extract it and then convert it for its use in a higher speed than it is replenished. The reserves of this material took millions of years to form, and it will take millions of years to replace the supplies used. Mining operations and, in particular, the mining method that it is being used in the quarry presented for this study carries a big production of waste material as well as lower mining recovery, nevertheless necessary to ensure safety conditions, but that will increase the unit cost. Having said all of the above, a solution is presented in this work, following the steps of the circular economy trend, where waste rock is being used both to lower the impact that wastelands have on the environment and to use this material as a aggregate for a rockfill that will eventually be used in the underground method and will finally allow a higher mining recovery.

This work should deliver a contribution for the geomechanical stability of marble underground exploitation. For that, an intense 3D numerical analysis, based on Finite Element Method is performed, using a real case study, where an hypothetical underground marble extraction is considered. Given the importance of the environmental costs of this kind of industry, a solution of backfill is analyzed.

1.2. Scope

The scope of this work is to analyze and understand the possibilities of mining recovery through a sustainable way that implies the reutilization of waste material and operational optimization. The work lead in this study will cover the simulation, using Finite Element Method (FEM) software, of stresses and strains in a drift, the mining design for the room and pillar method in a lower level and the safety conditions that will ensure structural and operational feasibility. As well as a stability analysis for the rockfill sequence that will be used to hold as new pillars and in which way will favor the pillar recovery.

The structure of this work will be presented in the next scheme:

In Chapter 1 a presentation of the work such as its objective and scope are introduced. In this chapter the extent of the thesis in order to structure it and organize it are presented. The scope has the mission of present the different procedures and stages needed to accomplish to report back to the objective of the study.

In Chapter 2 the literature review referred to the thesis work is presented. Here different topics that affect the condition of the study are discussed and analyzed in order to acknowledge the scientific research and for a better understanding of the own case study that will be completed in further chapters.

In Chapter 3 the case study is presented as well as its most intricate definitions that will play a role when applying the methodology.

In Chapter 4 the methodology and most practical part is explained in a way that captures the main objective of this work. It will present the approach taken towards the case study, where the problem is aimed as well as the research objectives and the calculation tools used in this study.

In Chapter 5 results from the simulation are presented and interpreted to reflect in detail the situation of the presented excavation.

In the last chapter, some final conclusions reflect a little bit on the discussion of the results, complementing with some observations that may be relevant for future studies within the scope of this dissertation.

2. Literature review

2.1. Quarry characteristics

A quarry can be defined, in terms of its typology, based on the following three parameters (Palma Guerreiro, 2000):

- Type of excavation: Underground or open pit;
- Geomorphological location: Plain or mountain;
- Quarrying method: One or more levels.

The shape of the quarry is determined by the morphology of the mineral deposit and the its accessibility. This characteristic can have a considerable influence on the type of machinery to be used, the cost and production characteristics (Palma Guerreiro, 2000).

The placement of a quarry is a function of the geomorphological environment where it is located. This location can take place on a more or less flat terrain (plain) or in an area of more or less accentuated topography (mountain). Lowland quarries, such as those in the Alentejo, develop in a pit or well, presenting advantages in environmental terms, due to the fact cavities are barely visible, but are penalized due to the impacts caused by their heaps. The location of a quarry on a mountain can assume three situations different; at the foot of the mountain, in the middle of its slope or at the top, assuming any one of them different conditions of access, transport, placement of waste rock, impacts production, among others.

The quarrying method defines the sequence of operations that allows the production of blocks. The method is established according to the characteristics of the mineral deposit (possession, orientation and inclination of the layer to be dismantled, among others) and the need for production, influencing significantly the type of machinery to be used and the logistical organization of the area to be explored. The explotation can be carried out on a single level or on several levels, the height and number of which are essentially a function of the layer to be explored and / or the fracture degree

present in the deposit, respecting the safety rules and the current legislation (Direção Geral de Energia e Geologia - DGEG, 2016).

2.2. Underground stone quarrying

2.2.1. Considerations

Quarries are typically and in its most general form, exploited by open pit methods, but there are several cases in which this can shift to underground methods, as seen as in countries like Italy, Croatia, Portugal, Greece and France among others.

Underground stone quarrying is a great alternative to typically open pit quarries that for technical, economical or environmental reasons can no longer operate as such. In general, underground quarries imply a higher cost and less mining recovery (Herrera, 2007) due to the quarrying method, typically this being room and pillar, as it allows higher recovery (Oggeri & Oreste, 2015). In order to continue with the exploitation, via underground methods, some parameters have to be revisited so underground excavation is feasible. First of all, marble's value is to be defined by the following aspects:

- Rock: color, texture, grain size;
- Rock mass: thickness, dip, reserve volume;
- Surface characteristics: weathering, vegetation, soil;
- Geography location: logistics;
- Market.

Underground quarrying is already, despite its higher cost, an excellent alternative when restrictions appear. Anyhow, the applicability of changing the exploitation method will also depend on restrictive factors, such as (Herrera, 2007):

- Economical, when sterile and coverings are important, quarrying ratio translates into high costs;
- Environmental, in areas of high ecological value, the underground method causes less environmental impact than in the open pit;
- Climatic, underground exploitation fronts are not affected by changes in seasons do not affect production.

Until 2016, the EU as a whole was the dominant producer and exporter of marble, but strong growth in emerging markets, especially in China, Pakistan and India, turned the tables and Asia is taking over as a producing and exporting region. In 2016, the world production of marble reached 816 million square meters. The world's top ten natural marble producers include China, India, Iran, Turkey, Italy, Spain, Brazil, Egypt, Portugal, and Greece (Focus Piedra, 2019). As for Portugal, most exploited marbles colours are white 'Branco Estremoz', pink 'Rosa Portugal', blue 'Azul Lagoa' and 'Ruivina' and finally, green, 'Verde Viana' (Bradley, 1999)

And third, there will be technical and operational factors that very much condition underground quarrying:

Operating methods chosen based on the geomechanical characteristics, start-up costs, infrastructure, rock characteristics, etc. In general, the use of the method of room and pillars is frequent;
Selection of the machinery: the use of equipment very similar to those use on open-pits is frequent, due to the advantages of the standardization of spare parts with other opencast quarries, a lower investment cost, a greater experience in handling and maintenance of machinery, greater availability of equipment used, greater production capacity per unit of capital invested, etc;
Access to the quarry through tunnels or ramps, since the wells are practically not used due to their high investment and development costs, although there are some known cases with the latter type of infrastructure.
Support technique (bolts, anchor cables, bolted plates, gunite, etc.) depending on the characteristics of the rock and the proper dimensioning of the pillars.
Ventilation, well sized for the rapid evacuation of fumes and gases generated by the operation of mechanical equipment and blasting.
Future uses of the underground space created, which can offset operating costs superior and complete mining projects with more rational uses. Generally, open cavities have as their most significant characteristics a practically constant temperature throughout the year, a location near or under densely populated areas and with a considerably high economic value of the soil, a reduced flow of groundwater when the rock mass have discontinuities, etc. Therefore, many underground quarries are being used for purposes as diverse as the storage of hazardous substances, the construction of parking lots, workshops, warehouses, offices, etc. The stability features in this particular type of void should be ensured on a long-term basis, without significant contribution from artificial supports.

2.2.2. Underground quarrying method

The main methods of underground exploitation are based on three distinct mining techniques, namely (Palma Guerreiro, 2000):

Artificial/Supported methods - the stability of the massif after excavated is ensured by the filling of the cavities.

Caving methods - the material is excavated through the controlled rupture of the rock mass as the voids increases.
Unsupported methods - abandoned rock pillars are left to guarantee the stability of the rock mass.

In general, to select the underground exploration method to be adopted, several factors such as the following need to be considered:

- Geological characteristics of the site;
- Morphology;
- Thickness and inclination of the marble layers;
- Continuity of the deposit;
- Depth ;
- Economic factors (infrastructure, initial investments, etc).

Only after obtaining information on the aspects mentioned above, should one proceed with the choice of the mining method to be used, as well as the design of it. As for marbles, exploitation feasibility is heavily influenced by block size (Oggeri et al., 2001). Since the cut and fill and block caving methods are more likely to induce fractures into the material, room and pillar seems the best choice, also because it allows a high recovery (approximately 70%) (Palma Guerreiro, 2000), given the block-shaped condition. This method, for underground stone quarrying, is also the most usual around quarries of this kind (Ravaccione and Fantiscritti quarries, in Italy; the Danby quarry, in Vermont, U.S. for example).

The design of the excavation for an underground quarry usually comes from an open pit exploitation. For this quarrying method open-pit and underground exploitations are combined, being carried out in depth. Generally, there is already an open pit, however, it may happen that in any given direction of the excavation, this does not prove to be feasible, starting an underground exploitation.

Room and pillar mining is applied to minimize surface subsidence and damage of the overlying strata, it is also advantageous because it can be mechanized, and is relatively simple but is connected with mining losses. It is a mining system in which the mined material is extracted across a horizontal plane, creating horizontal arrays of rooms and pillars . To do this, "rooms" of stone are excavated while "pillars" of untouched material are left to support the overburden roof (Kim et al., 2018). The technique is usually used for relatively flat-lying deposits, such as those that follow a particular stratum in the case of ore deposits, or have spatial continuity and competency. Pillars are the stabilizing elements inside the room and pillar mining scheme (Figure 2). Therefore, dimensioning pillars in conjunction with roof stability of chambers are the key issues from the geomechanical point of view (Schleinig & Konietzky, 2017).

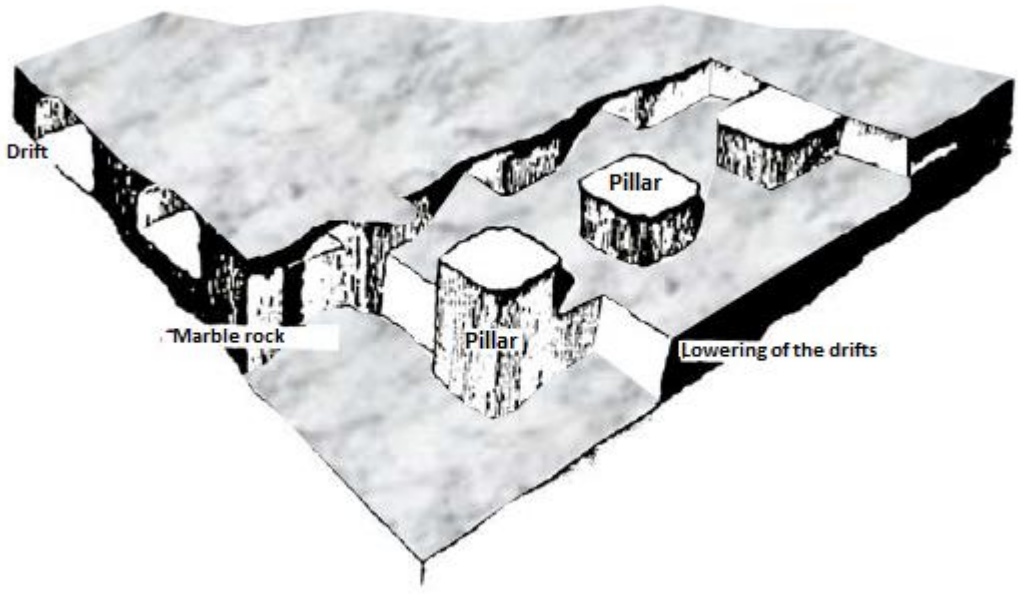

Figure 2. Layout of a room and pillar excavation (adapted from Palma Guerreiro, 2000).

The underground exploitation occurs in two distinct stages, the opening, with the excavation and enlargement of the tunnel; and the lowering, with the mining of the chambers through gradual lowering.

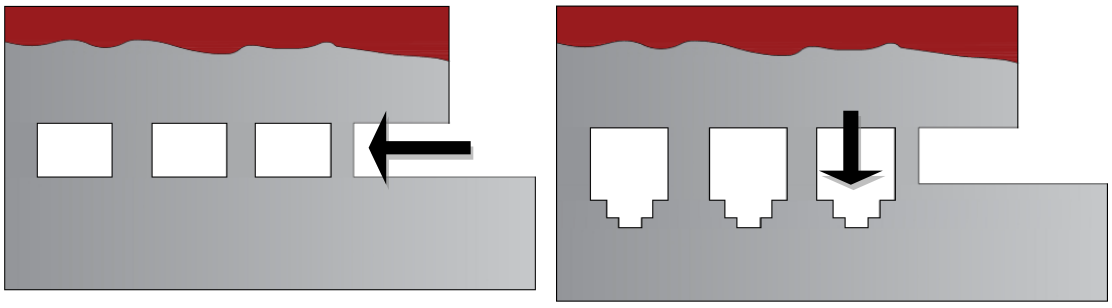

Figure 3. Phase 1º (left) and 2º (right) of the room and pillar excavation.

It starts from the horizontal level of the open pit exploration and then it continues from the first advancement gallery (typically 5 to 6m x 3 m), the exploitation is laterally leaving the pillars to sustain. After exploiting horizontally, it continues by exploiting in depth (Figure 3) (chamber height usually goes up to maximum 50 m) (Esterhuizen et al., 2011).

The extraction techniques used in the second stage, that is, from the development at the top to the squaring of the blocks, are the same as those used for open pit mining, contrarily, the excavation of top tunnels anticipates specific techniques. The advancement operation is usually done both with a chain saw and a diamond wire cutter. A smaller portion of the rock is isolated using a hydraulic jack and then the cut is performed behind using a four-pulley return frame. A remarkable advantage of this method is the ability to control the direction of the cutting, leading to the possibility to perform a selective extraction.

Most of the marble quarries and other types of ornamental rock, with underground exploitation, use room and pillars mining methods, essentially due to the following aspects (Herrera, 2007):

- The supporting elements are the pillars (cheaper);
- The columns can be dimensioned so that there are no fractures induced in the rock mass (safety factor safeguarding the integrity of the mineral deposit of the point view of fracture);
- They generally allow an acceptable recovery (between 60 - 90%);
- There is the possibility of leaving pillars in areas where the material is not so good quality;
- Most open-air equipment can be used, as it allows large dimensions.

In spite of the advantages, there are also some disadvantages that need to be considered (Herrera, 2007):

- High production and investment costs;
- Geometric constraints in the excavation due to the need to maintain stability;
- Need for detailed knowledge of the geological and geotechnical characteristics of the deposit;
- Need for ventilation, lighting and sewage.

2.3. Mining Recovery: Room and Pillar backfill

The circular economy concept advocates drastically reduced primary resource extraction in favor of secondary material flowing through internal loops. However, it is unreasonable to think that society will not need any resources, for example, metals, from mining activities in the short, medium, or longer term. Mines can make significant progress if they apply the circular economy principles at the mine site level. Circular flows within the economy aim at keeping resources in use for as long as possible and limit final waste disposal. Likewise, operating mines for as long as material can be extracted at acceptable environmental costs, thus minimizing the loss of a nonrenewable resource, can be viewed as a contribution of the mining industry to circular economy objectives (Lèbre et al., 2017).

The exploitation of quarries comprises an important part of the mining industry with the objective of providing with construction materials that are extracted. This type of mining is characterized by the creation of a strong impact on the environment, hence the need to know the different aspects necessary for the correct exploitation of a quarry. Therefore, a green mining method has been widely promoted and applied to scientifically solve the above issues.

2.3.1. Pillar recovery

Although the room and pillar mining method is structurally sound, it decreases the life of the mine because approximately 25 % of the resource is not used (Tesarik et al., 2009) an according with Herrera (2008), not used resources can go from 10% to 40%. Many mines all over the world have

included the technique of backfilling the stopes created in the room and pillar method and consequentially recovering the ore pillar, in some cases, to its totallity. Many examples can be seen in other countries such as the Keretti Mine in Finland (Kojo et al., 2013), the Cannington mine in Australia (Sivakugan et al., 2015), the Magmont mine is the United States (Tesarik et al., 1995), with complete recovery of previously developed room and pillar mines, and in mines around Canada among others.

Backfilling has important benefits such as improved regional and local rock stability through the support provided by the backfill, reduced costs of building significant tailings disposal structures on the surface, and the reduced environmental impacts by the underground containment of waste material (Oldecop & Alonso, 2013). The sequence of creating these new pillars and remove the valuable ones follows a process that might vary for each case but primarily it follows the basic steps of firstly, defining the area of backfilling and pillar recovery within the underground exploitation layout, previously studied; secondly, closing of this area in order to fence in the backfill as well as the construction of a backfilling retaining wall between two adjacent room pillars; thirdly, the actual backfill through pipelines is laid within these retaining walls and some monitoring gauge can be placed within the new pillars; finally the valuable pillars are removed with its correspondent monitoring and analysis to ensure that the new pillars are in fact competent (Zhou *et al*, 2019). With this one backfilling cycle is completed and the operation can be moved onto another selected area.

To recap, backfill recovery of residual room pillars is the utilization of the supporting strength of a backfilled structure in place of the supporting strength of the residual ore pillars, thereby achieving the recovery of said pillars (Zhou *et al*, 2019).

As for marble underground openings, they have a medium to high potencial suitability to hold waste rock material, having in mind their relative permeability and the material thickness above them (Campo et al., 2018).

2.3.2. Types of backfill

Backfill refers to any waste material such as tailings, sands or waste rocks that is placed into the underground mined voids (stopes) for the purposes of either disposal or to perform some engineering function. Backfills that are used only to fill the voids created by mining need only to have sufficient strength to prevent any form of remobilization through liquefaction, typically caused by dynamic loading. However, where backfills are used as engineering materials, sufficient strength is required to ensure stability during exposure during ore pillar mining in tall vertical faces or undercuts (Alonso et al., 1990). Backfills can be divided into two broad categories, cemented or uncemented.

Cemented backfills include a percentage of pozzolanic binder such as cement, fly ash etc. to improve the strength. This category includes:

- Cemented rock fills (CRF);
- Cemented aggregate fills (CAF);

- Cemented hydraulic fills (CHF);
- Paste fills (PF).

The Uncemented (unconsolidated) consists on waste material dumped into the stope void. As its name indicates, this type of backfill does not use any type of binder. The most typical unconsolidated fills are:

- Hydraulic fills (HF);
- Rock fills (RF);
- Sand fills (SF);
- Aggregate fills (AF).

The rock fill consists of gravel size to boulder size materials. The abundance of the rock fill material from the previous operations dictates the selection of rock fills over any other type of fill. In a marble quarry, this type of backfill material is in abundance in wastelands. However, when backfills are used as engineering materials, sufficient strength is required to ensure stability during exposure during ore pillar mining in tall vertical faces or undercuts, particularly in the case of paste fills or other cemented fills. The best option then, when pillar recovery is desired, is to appeal for cemented rock fill (CRF) (Sivakugan et al., 2015).

Cemented backfill enhances the strength to help along with stresses that can occur when recovering the residual pillar. Anyhow, using CRF as a backfill technique needs a series of studies and considerations in order to find a feasible way to carry it. In one hand, it will allow waste material from the quarry to serve as an operational leverage as it both benefits environmental aspects and mining recovery. On the other hand, cement brings along economic and environmental complications. In addition to the large carbon footprint associated with the cement production, due to the high transport cost to the mine site cement adds significant cost to the backfills, even in such small dosages in the order of 3–6 %. One solution that the mines have been trying is to replace cement with blended cements, which consist of cement mixed with fly ash and/or slag, with considerable success (Rankine et al., 2007).

2.3.3. Waste rock

Waste rock is typically removed during mining operations along with overburden and often has little or no practical mineral value (Federal Highway Administration, 2016). In the case of marble quarrying, this waste rock is generated in every situation where the blocks do not follow, not only specific parameters related with, e. g., color, texture or grain size, but also by the conditions of these blocks, e.g. if the block size is too small for the market parameters or it is very weathered. When considering waste rock for possible uses, such as an aggregate for cemented rockfill, its physical properties need to be evaluated. Waste rock generally consists of coarse, crushed, or blocky material covering a range of sizes, from very large boulders or blocks to fine sand-size particles and

dust. Physical properties such as hardness or density need to be considered as well as global properties for the rock fill such as grain size distribution.

2.3.4. Cemented rockfill mechanics

The mechanical stability of cemented waste rock under compression is usually of concern, as it is under pressure throughout the service period, mainly from four aspects: cementing materials, aggregate particles, additive materials, and environmental conditions.

Concerning **cementing materials,** (including its type, content, and even the mixed formulation of multiple cementing materials), it is believed that the mechanical parameters of cemented waste rock can be increased by improving its bonding performance. The typically used binder is the Portland cement, but others can be used to decrease the content of this Portland cement, with a large carbon footprint, such as pozzolanas.

The **aggregate particles**, which include particle composition, content, and particle size distribution, it is considered that the internal structure of backfill can be strengthened by reducing the elements that can deteriorate the hydration product and optimize the spatial distribution of the particles.

A**dditive materials**, including nanomaterials, polymers, fibers, alkaline substances, and water-absorbing substances, it is believed that the hydration process can be improved, the formation of hydration products can be promoted, and even more reliable links can be generated at the cement-rock boundaries to optimize the loading structure of backfill.

Finally, the **environmental conditions**, including temperature, corrosion, conservation, and stress field, it is considered that creating more favorable environmental conditions can improve the mechanical properties of cemented waste rock.

From the literature available, many examples of CRF can be found (e.g. Shrestha et al. (2008); Warren et al. (2018) or Wu et al. (2018)) and in them, where the global properties for this technique are presented. In the Shrestha et al., 2008 study on the the Diavik Diamond mine in Canada CRF procedure it examines the physical properties of the cemented rock fill such as densities and moisture, cement content and cement/ water ratio and specific gravity and relates it with the unconfined compressive strength. Warren et al., 2018 focused on the strength and mechanical parameters of CRF for backfilling and Wu *et al*., 2018 focused their study on particle size distribution of CRF. From this literature main CRF parameters and composition can be taken out:

Grain size analysis. From Wu *et al,* 2018 testing of different grain sized aggregates of the CRF were tested to quantify its effect on the mechanical parameters. For this the Talbot gradiation was used. It is a continuous exponential gradation, which is conductive for characterizing the particle distribution of the aggregate in cemented rockfill (Talbot & Richart, 1923; Zhou et al., 2019). Its function is [1]:

$$P = \frac{M_c}{M_t} = \left(\frac{d_c}{d_{max}}\right)^n \quad [1]$$

Where P is the mass ratio; d_c is the current size of the particles; d_{max} is the maximum size of the particles; M_c is the mass of the particles below or equal to dc; M_t is the total mass of the particles; and, *n* is the Talbot index. After the mechanical parameters are calculated (the strength parameters of cohesive force, internal friction angle, and tensile strength can be obtained, being based on the Mohr-Coulomb strength criterion) a relationship is obtained were maximized mechanical parameters are sought within a range of the Talbot indices that give the mass distribution of the particles in the cemented rockfill specimens (for Wu et al, 2018, this range is 0,4-0,6; for Shrestha et al, 2008 the Talbot index is 0,5). Afterwards, this was put to the test on numerical techniques modeling to simulate displacement and stresses of the strata when the backfill is placed. The results showed that optimizing the particle size distribution of the aggregate in cemented rock fill could increase the loading capacity of the backfill to improve the filling effect, effectively control the strata movement, and decrease the stress of the rock mass. It is also important to consider that coarse particles undergo crushing and breakage more than fine ones (Alonso *et al*, 1990).

Physical properties. The Shrestha et al, 2008 study shows that a 6% cement content resulted in an average 28-day UCS of 11.5 MPa versus 8 MPa for 5.5% both with a water – cement ratio between 0.98 and 1.10. Literature indicates that the usual cement content is 5% to 7%. The variation of dry density with moisture content for a given compaction effort of the mixing equipment indicates that a moisture content between 5 to 8% gives a higher density, and that a moisture content of around 7% provides optimum compaction. CRF compaction also has a significant impact on strength, an 8% increase in the density of a CRF sample from 2082,4 to 2242,5 kg/m^3 (Warren *et al*, 2018), may cause an increase of nearly 60% in the UCS test result. So to achieve high density samples more compaction is required but it might result in more particle breakage as coarse particles undergo crushing more than fine ones. Particle breakage leads to a reduction of peak strength and stiffness.

Mechanical parameters. Uniaxial Compressive Strength (UCS), elastic modulus, poisson's ratio, cohesive strength, friction angle and tensile strength. The purpose of the study of these parameters is to determine the strength and mechanical properties of the backfill after curing 28 days to design safe undercut spans that ensures that the emplaced strength of the backfill exceeds the strength required to support its own weight and resist applied loads from the surrounding rock mass. According to Warren et al, 2018, UCS can vary with the following parameters: density (as seen above); wet-screening, as in removing the oversized aggregate when preparing the samples, effectively changes the mix design, increasing the cement-to-aggregate ratio (Neville, 2009) that produces a relative increase in strength as compared to the emplaced strength of the bulk material; particle size effect (as seen above) and age: The UCS test (ASTM C31/C31M) results indicate that the strength of CRF continually increases with time, but that the rate of strength gain gradually diminishes with prolonged curing time. Because most underground mines provide favorable curing conditions, the in-place CRF should continue to gain strength. However, as with concrete, if the relative humidity drops below 80% or the temperature drops below freezing, the hydration process

may be halted (Kosmatka et al., 2002). As for the Elastic properties Warren *et al,* 2018 estimate the following values in Table 1, for the friction angle they follow the Mohr-Coulomb theory using range of friction angles and they assume σ_t can be calculated as a 10% of UCS.

Table 1.Strength and Elastic properties deducted from literature.

Property	Warren et al, 2018	Shrestha et al., 2008
UCS σ_o (MPa)	3,44 – 6,55	4 – 7
Tensile strength σ_t (MPa)	0,34 – 0,65	
Cohesion c (MPa)	0,68 – 1,72	0,8 – 1,7
Friction angle Φ	35º- 45º	40º
Modulus E (MPa)	1 378,9 – 5 515,8	2 000 – 3 500
Poisson's ratio υ	0,16 – 0,25	0,2 – 0,3

Regarding the mechanical behavior, Oldecop & Alonso, 2013 summarized that two different features can be looked at: time dependent deformations and collapse deformations. Collapse strain increases with stress almost linearly for most rock fill materials. The collapse phenomenon does not tend to vanish under high stresses, as observed in soils. From the points explained above, the collapse deformation increases for:

- Weaker rock particles;
- Larger particle size ;
- Grain size uniformity;
- Less compaction;
- Lower initial moisture.

All these observations are consistent with the hypothesis relating collapse with particle breakage. For this particular study, particle breakage will not be studied further but proposed for further works on the topic.

2.4. Underground stability analysis

2.4.1. Considerations

Previous works have been executed on the possibility of going underground in the Estremoz basin quarries, among others, Almeida & Nunes Costa (2000), Oggeri et al. (2001) or Costa e Silva (2002). According to Oggeri et al. (2001), the pit quarries in the Alentejo region have two types of problems. The first is a geo-mechanical one, and it is linked to the redistribution of stresses under the new

geometrical configuration, where a lateral confinement is no longer applied and therefore the instability of lateral walls is possible when discontinuities occur in unfavorable orientation.

The second is a technical and economic problem when changing the excavation method to underground extraction. In this case, the underground channels are excavated directly in the productive and massive rocks, avoiding the removal of overburden. According to the study, it is necessary to maintain stable structures in the rock (rib pillars and eventually thick horizontal beams) without excessive loss in block recovery.

The application of tools and models in rock mechanics to underground exploitations is justified for safety reasons, guaranteeing the stability of the exploitation in relation to workers, and for economic reasons, by controlling the deformation and excavation of the ground in order to prevent the disruption of the work. For the room and pillar method several works have studied the stability that requires this type of exploitation to ensure safety, either for both equipment and workers or environmental (Direção Geral de Energia e Geologia - DGEG, 2016) . In order to produce a reliable simulation on the model, it is important to quantify the parameters that will eventually condition the analysis. A stability analysis is the key to understand how the model will react to the given conditions. In general terms and according to Correa (1991), the main factors affecting mining stability are:

- The field stresses;
- The strength, deformability and other mechanical properties of the layers;
- Groundwater conditions;
- The method and quality of the excavation;
- The underground support system;
- The interaction between adjacent underground excavations.

When assessing the efficiency or limitations of numerical techniques in mining, three stages should be considered related to modeling: the development of the model, the application of the model and the validity of the model. At essence, for mining purposes, there is today a wide range of possible modelizations available both in two and three dimensions as well as constitutive models for many material behaviors: linear elastic, non-linear elastic, visco-elastic linear, anisotropic, orthotropic, dilating, stochastic, etc. The evaluation of stress distribution, around the underground openings, is important for designing a proper support system and must incorporate (diverse) material properties, presence of discontinuities, non-homogeneity and state of in situ stresses existing in the rock mass.

In addition to this, nonlinear constitutive behavior of the rock mass and potentially large strain deformations must also be considered. In such a situation, finite element analysis is found to be quite efficient in handling such complexities.

2.4.2. Numerical techniques available for geomechanical modeling

When finding solutions to a geotechnical problem, three main methods can be considered. The first ones are the empirical methods that evaluate the stability of the mining infrastructure through statistical studies of underground conditions which are supported in the practical experience and judgment of the engineer. The second one being observational methods were continuous monitoring is required (Correa, 1991). The third method considers the numerical methods. The use of numerical methods in modeling and simulation of rock masses and excavations is widely used given its efficiency for the determination of approximate solutions. Inside these techniques there are four that stand out when having a geotechnical case study: the Finite Element Method (FEM), the Finite Difference Method (FDM), the Discrete Element Method (DEM) and the Boundary Elements Method (BEM).

The FEM has its origin from the need to solve complex elasticity problems and structural analysis of civil engineering and aeronautics. Developed by Courant (1943) it provides with an essential feature: discretization mesh of a continuous domain in a set of discrete sub-domains, generally called elements. Discretization involves dividing the geometry into a number of finite elements (mesh) to solve second order partial differential equations (PDE). The method has already been generalized for numerical modeling in a wide variety of engineering disciplines, for example electromagnetism, transfer of heat, and fluid dynamics (Martinez, n.d.)

FDM is another numerical method to solve differential equations, approximating them with difference equations, in which the finite differences are approximated from the derivatives. FDMs are, therefore, discretization methods.

The Discrete Element Method (DEM) it is used to calculate the motion and effect of a large number of small (discrete) particles. The discrete element method is related to molecular dynamics, but it differs due to the inclusion of degrees of freedom (movements) of rotation, contact between the discrete elements and, frequently, complex geometries used to define them.

BEM is a computational method for solving systems of differential equations, formulated in an integral way. It is applied in various areas of engineering, such as fluid mechanics, acoustics, electromagnetism, and fracture mechanics (de Araujo & Pereira, 2017).

Despite the differences in the set of available numerical methods, the correspondent analysis follows a general three step process. First the modeling has to be done, which is the visualization of project sections. Modeling process includes:

- Creation of geometry;
- Definition of edges;
- Definition of Material and structural properties;
- Mesh generation;
- Allocation of Loads;

- Assignment of boundary conditions.

the first step is followed by the calculation stage, where several processes happening to the model are examined. Such processes can be from deep foundations and soil-structure interactions, the analysis of tunnel boring (TBM) considering sequences to slope stability and groundwater flows.

Finally, results are presented and ready to assess them in a graphical, diagram or tabular format. Parameters such as displacement, force, tension, deformation can be read. This step is also known as the postprocessing stage.

Another very important aspect in what concerns to numerical modelling is the input data. It is crucial to list the geotechnical parameters that are important for the determination of the stability of underground excavations:

- Orientation of the discontinuities in the rock mass;
- Spacing of these discontinuities;
- Condition of the discontinuities including roughness, separation, persistence, weathering and filling;
- Characteristics of groundwater;
- In situ state of stress;
- Strength and deformability of the in situ rock mass material.

Generally, for the application of this method to the solution of practical engineering problems, the following parameters are required: geological conditions of the site under consideration, relevant properties of the rock masses (deformability or stiffness of the site) and boundary conditions (in-situ stresses) (Correa, 1991).

Having mentioned all the parameters to consider when applying a numerical method to start with a stability analysis, previous data has to be collected. Collecting this data comes from an exhaustive characterization of geomechanical features, which at the same time can be divided onto a geo-structural analysis, by pointing out families of discontinuities; and a mechanical characterization, by running tests on samples. These mechanical characteristics of the rock are applied to the entire model.

2.4.3. The Finite Element Method

The Finite Element Method is a numerical technique for solving problems that are described by partial differential equations or can be defined as functional minimization. Approximating functions in finite elements (domain of interest represented) are determined in terms of nodal values of a physical field which is sought. A continuous physical problem is transformed into a discretized finite element problem with unknown nodal values. For a linear problem, a system of linear algebraic equations should be solved. Values inside finite elements can be recovered using nodal values (Süli, 2019).

In general terms, the basis of the finite element method corresponds to the definition of the domain of a problem surrounding an excavation and the division of that domain into a set of discrete and interacting elements. The steps needed to endeavor such operation are listed below (Nikishkov, 2004):

1. Discretize the continuum. First, a solution region divides into finite elements. The finite element mesh is typically generated by a preprocessor program. The description of mesh consists of several arrays main of which are nodal coordinates and element connectivities (*Figure 4*).

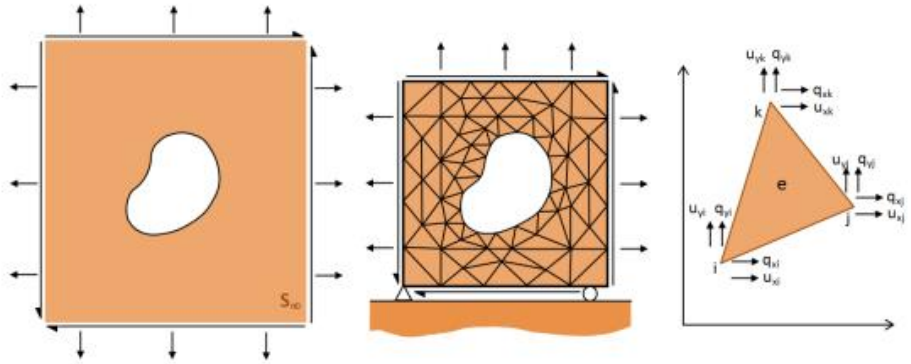

Figure 4. Depiction of the discretization of the problem into finite elements (in Paneiro (2014*), adapted from* Brady & Brown (2006)*).*

2. Select interpolation functions. Interpolation functions are used to interpolate the field variables over the element. Often, polynomials are selected as interpolation functions. The degree of the polynomial depends on the number of nodes assigned to the element.
3. Find the element properties. The matrix equation for the finite element should establish a connection between the nodal values of the unknown function to the problem properties. In order to do this, different approaches are used; the most convenient are: the variational approach and the Galerkin method. If the physical expression of the problem is known as a differential equation then the most popular method of its finite element formulation is the Galerkin method. If the physical problem can be formulated as minimization of a function then variational formulation of the finite element equations is usually selected.
4. Assemble the element equations. To find the global equation system for the whole solution region, all the element equations must assemble. In other words, local element equations need to combine for all elements used for discretization, for this operation, element connectivities are used. Before the solution, boundary conditions (which are not accounted in element equations) should be imposed.
5. Solve the global equation system. The finite element global equation system is typically sparse, symmetric and positive definite, to solve it direct and iterative methods can be used. The nodal values of the sought function are produced as a result of the solution.
6. Compute additional results. In many cases we need to calculate additional parameters. For example, in mechanical problems strains and stresses are of interest in addition to displacements, which are obtained after solution of the global equation system.

As said before, the FEM bases on a solving a problem that is described by partial differential equations. The first step in FEM is to identify the partially differential equation (PDE) associated with the physical phenomenon. The PDE (or differential form) is known as the strong form and the integral form is known as the weak form. PDEs can be categorized as elliptic, hyperbolic, and parabolic. When solving these differential equations, boundary and/or initial conditions need to be provided, such boundary conditions (B.O.) are the Neumann or natural B.O. (represented as Γ_N in *Figure 5*) and the Dirichlet or essential B.O. (Γ_D in *Figure 5*). Based on the type of PDE, the necessary inputs can be evaluated (Harish, 2020).

Secondly, the discretization of the domain Ω (*Figure 5*) is divided into finite elements connected at nodes. Shape functions Ni are used for interpolation of certain property inside a finite element.

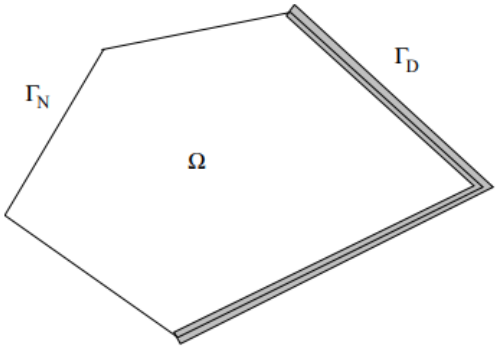

Figure 5. Representation of the problem domain and the boundary conditions (Sayas, 2008).

Considering some abstract three-dimensional finite element having the vector of nodal displacements $\{q\}$ [2]:

$$\{q\} = \{u1\ v1\ w1\ u2\ v2\ w2 \ldots\} \qquad [2]$$

Displacements at some point inside a finite element {u} can be determined with the use of nodal displacements {q} and shape functions *Ni,* Interpolation functions are defined for each element to interpolate, for values inside the element, using nodal values (Sayas, 2008). These interpolation functions are also often referred to as shape or ansatz functions [Ni] [5]. Thus the unknown {q} functional can be reduced to [3]:

$$u = \sum Niui$$

$$v = \sum Nivi \qquad [3]$$

$$w = \sum Niwi$$

These relations can be rewritten in a matrix form as follows [4]:

$$\{u\} = [N]\{q\} \qquad [4]$$

$$[N] = \begin{bmatrix} N1 & 0 & 0 & N2 & \dots \\ 0 & N1 & 0 & 0 & \dots \\ 0 & 0 & N1 & 0 & \dots \end{bmatrix} \quad [5]$$

Strains can also be determined through displacements {ε} at nodal points [6], expressed through a displacement differentiation matrix that can be obtained by differentiation of displacements expressed through shape functions and nodal displacements.

$$\{\varepsilon\} = [B]\{q\} \quad [6]$$

[N] is a matrix of shape functions and [B] is the displacement differentiation matrix. Using Galerkin method, the weak form can be rewritten and reduced to a matrix form [7] (Courant, 1943):

$$\{F\} = [K]\{U\} \quad [7]$$

{F} is a known action (loads, force, heat source, etc);

[K] is a known property (geometry, stiffnes, etc) also known as stiffness matrix;

{U} to be determined (displacements).

This can be solved mathematically using a matrix inversion method [8]:

$$\{F\} = [K]\{U\} => \{U\} = [K]^{-1} \{F\} \quad [8]$$

Once the {U} displacements are known, the stresses and strains can be determined [9]:

$$\varepsilon = \Delta/L \quad [9]$$

The FEM analysis can be divided in three stages that differentiate the computational work from the engineering work. These three stages are the preprocessing, the processing and the postprocessing phases (*Figure 6*). The preprocessing stage corresponds with the creation of the geometry and the definition of the properties for said model. It also corresponds with the definition of the yield criterion and the type of mesh and restrains that the model is going to behave under. This part corresponds with approximately the 70% of the engineering effort. The processing corresponds to the calculations that the computer and system will make in order to come up with a solution for the problem stated. This corresponds with a 5% effort of the total. Finally the postprocessing corresponds again to an engineering work where the model is verify and data is collected. This phase corresponds to a 25 % of the total effort.

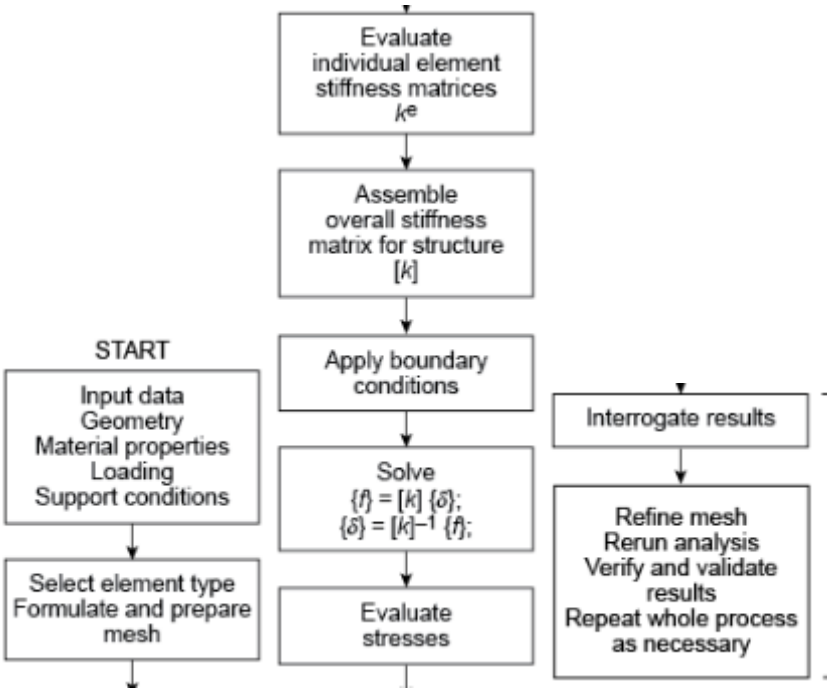

Figure 6. Finite Element Analysis procedure a) left picture, b) central picture, c) right picture (adapted from : OpenLearn, n.d.).

In order to determine the ultimate geotechnical strength i.e. the failure (or collapse) load from numerical analyses or analytical methods, we have to consider the rock's shear strength, and describe its non-linear response up to failure with a suitable material model. There are two ways to define the behavior of a rock when failure occurs: through the state of stress or through the state of deformation (González de Vallejo et al., 2002). The first one, often used, the maximum stress that the rock can support is taken as the resistance of the rock. For any point in the rock mass the stress tensor is defined by six components, three normal components, and three tangential components, σ_{xi}, σ_{yi}, σ_{zi}; τ_{xyi}, τ_{yzi} and τ_{xzi}, in a coordinate system (x, y, z). Depending on the magnitude and direction of the six components of the tensor, the three main stresses are obtained, σ_{1i}, σ_{2i}, σ_{3i}, where σ_{1i} is the major principal stress, σ_{2i} the intermediate principal stress and σ_{3i} the minor principal stress.

The use of a specific failure criterion to study a problem must satisfy the following requirements (Brown & Hoek, 1980):

a. Properly express the response of an intact rock sample to the range of tensions existing underground. These ranges of conditions go from tensile strength up to triaxial compression.
b. Being able to predict the influence of one or more discontinuity families on the rock sample behavior. This behavior can be highly anisotropic, that is, it will depend on the dip of the discontinuities in relation to the direction of application of stresses.
c. Enable the projection, even if approximate, of the rock mass behavior at scale, containing several families of discontinuities.

Depending on how the yield surface equation (f) is defined, different failure criteria are obtained. The first is a linear failure criterion called Mohr-Coulomb failure criterion, and the second is the Hoek & Brown failure criterion for non-linear equations. The simplest model used in practice is the elastic-perfectly plastic model combined with a Mohr-Coulomb failure criterion referred to as the Mohr-Coulomb model for brevity. The model is used to describe the real rock stress-strain response with an idealized elastic-perfectly plastic stress strain curve, which is direct to define as it requires the minimum number of input rock parameters. This criterion is going to set the yield criterion for this study and for that, it will be explained further.

The Mohr-Coulomb criterion is a linear failure criterion. This means that the equation defining the yield area is a linear equation. It is based on two properties of rocks and rock masses, the friction angle and cohesion. The function that defines is given by the tangential stress and normal stress in a plane. In this case the yield surface is of the form τ = f (σ). The mathematical expression of this equation is equation 10:

$$\tau = c + \sigma_n \ tan\varphi \qquad [10]$$

Where c is cohesion, φ is the friction angle, σ_n is the normal stress on the yield area, and τ is the tangential stress on the yield area.

According to this criterion the rock breaks by traction, according to normal planes in the direction of applied stress, or by shear cut, in planes where the difference between the shear stress and the action of friction angle is maximum. In addition, this criterion says that the friction angle of the material can vary for the same rock depending on the variation of confinement stress.

2.4.4. Pillar and roof Span instability in Stone Mines

In the room and pillar method the design of the excavation is based on the compromise between security and the maximum economic use of the mineral deposit. The roof span is required to remain stable during mining operations for haulage as well as access to the working areas as from literature, roof and rib falls account for about 15% of all reportable injuries in underground stone mines (Esterhuizen et al., 2011). The size of the rooms in underground stone mines is largely dictated by the size of the mining equipment.

Esterhuizen et al. (2010), developed a study for the identification of large block falls on underground stone mines across the U.S.. The authors also identified the most significant factor contributing to each fall:

Stress: High horizontal stress was assessed to be the main contributing factor in 36% of all large roof falls observed. These falls are equally likely to occur in shallow or deep cover. A roof fall related to stress-induced damage was observed at a depth of as little as 50 m (160 ft).

Weak bedding planes: The beam of stone between the roof line and some overlying weak band or parting plane failed in 28% of all observed large roof falls. Weak bands can also appear within pillars that can extrude resulting in progressive spalling of the pillar ribs.

Discontinuities: Large discontinuities extending across the full width of a room contributed to 21% of the large roof falls. Large angular discontinuities that typically extend from roof-to-floor in a pillar are also a major reason for failure and can significantly weaken them.

Weak roof rocks: The remaining 15% of the roof falls was attributed to the collapse of weak shale inadvertently exposed in the roof or progressive failure of weak roof rocks.

Designing an excavation should include parameters that ensure safety as well as technical feasibility and it should be directed using basic engineering principles (Esterhuizen et al., 2008): First, a geotechnical characterization is needed. Designing structures for stone mines can be successfully carried out if correct geotechnical investigations are conducted on the upper hand. Such investigations include rock strength testing, core logging, bedding layering assessment, joint orientation assessment, and rock mass classification. The maximum horizontal stress (magnitude and orientation) is also expected to be calculated to avoid further problems. Secondly it is important to have into account the rock mass quality, using the results of a rock mass classification or direct inspection of workings, confirming the rock strength and rock mass quality is key when studying stability of the rockmass. Following, the selection of mining direction should be favorably oriented to potentially high horizontal stress and the prevalent jointing. The image below shows possible scenarios for the excavations (Figure 7):

1. Between 45º - 90º. It is considered very favorable in terms of stability and favorable in terms of block design.
2. Between 20º - 45º It is considered favorable in terms of stability but unfavorable in terms of block design.
3. Between 45º - 90º. It is considered unfavorable in terms of stability but favorable in terms of block design.
4. Between 20º- 45 º. It is considered very unfavorable in terms of stability and unfavorable in terms of block design.
5. Between 20º - 45º. It is considered unfavorable both in terms of stability and in terms of block design.
6. Between 45º - 90º. It is considered both very unfavorable in terms of stability and in terms of block design.

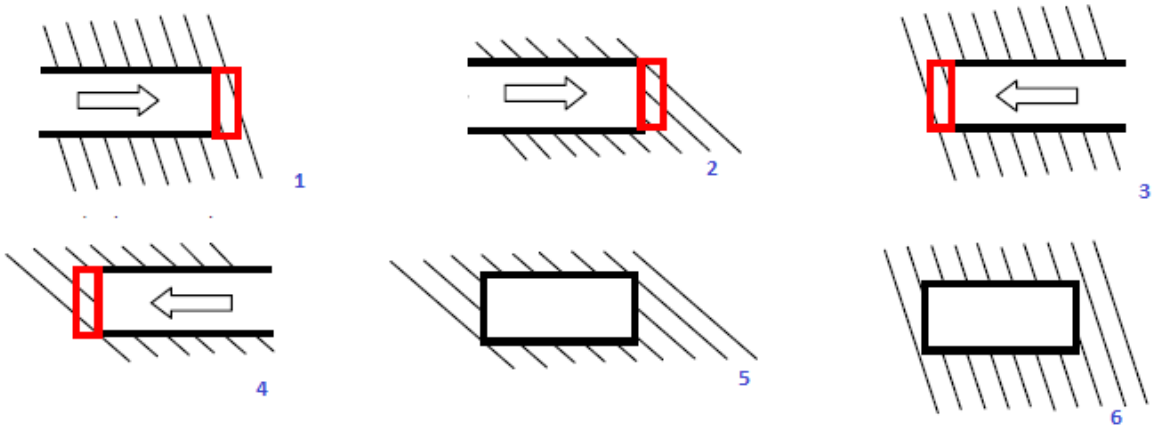

Figure 7. Layout of possible excavation situations given joint orientation (adapted from Palma Guerreiro, 2000).

Since room-and-pillar mines have two orthogonal directions of mining, the heading direction should be favored over the cross-cut direction when selecting the orientation of the layout. The heading direction should be oriented parallel to the direction of major horizontal stress, with due consideration of joint orientations and cross-cut stability (Figure 8). Often there will be a compromise to select the final heading orientation, when expected, to ensure stability.

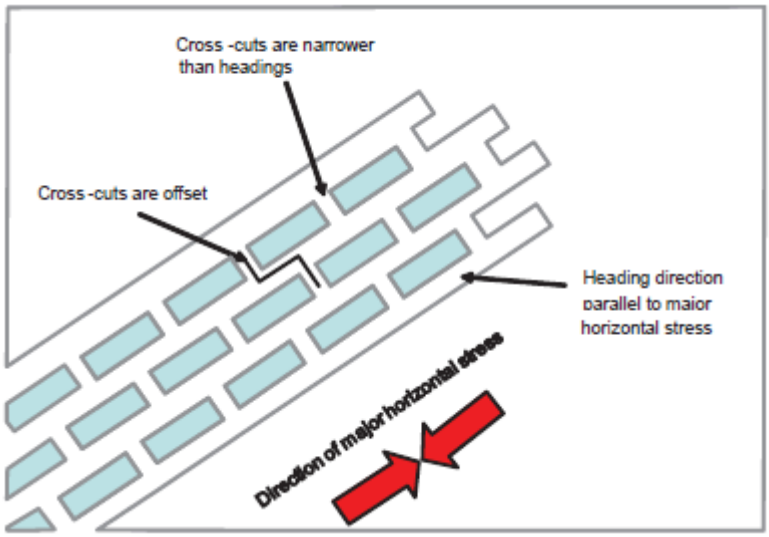

Figure 8. Layout of mining heading regarding major horizontal stress (Esterhuizen et al, 2010).

Roof thickness should be studied carefully and specially, lithology changes and bedding planes should be identified in order to select the beam thickness. Even though literature shows that an immediate roof beam smaller than 1,2 m is unlikely to be stable, horizontal stresses should be defined in order to select a higher thickness (Esterhuizen et al, 2010). Many of the mines that do not use roof supports have a natural parting as the roof line.

The roof span design is highly connected with rock quality, and even though literature showed that 10 to 15 m spans can be achieved, it is wise to select an initial span no longer that 12 m. Longer spans should count on monitoring and possible support.

Finally, support system and monitoring in the form of patterned rockbolts may be required if the conditions above are not favourable and once a roof design has been finalized and mining is underway, monitoring should be implemented to verify the stability of the roof.

3. Case study

In the Portuguese mining panorama, Alentejo marbles represent one of the most capable and proliferous resource and basically the biggest exploitation in the last sixty years (Carvalho et al., 2013). The superior quality of marbles has made possible since Roman times the use of this marble seen as in Roman monuments, not only from Portugal, but also from Spain. Alentejo lengthy history has provided Portugal with worldwide reputation on marble exploitation.

3.1. Location of the Quarry

The case study of this work is based on Monte d'el Rei MJ 5282 quarry, located in the area known as the "marble triangle" (Estremoz – Borba – Vila Viçosa) in Alentejo's northeast, between Sousel and Alandroal (Figure 9). This area contains Portugal's most important ornamental marble deposit, in terms of duration and profitability. In fact, Alentejo marbles have provide the region with economic benefits for a number of decades (Lopes, 2007).

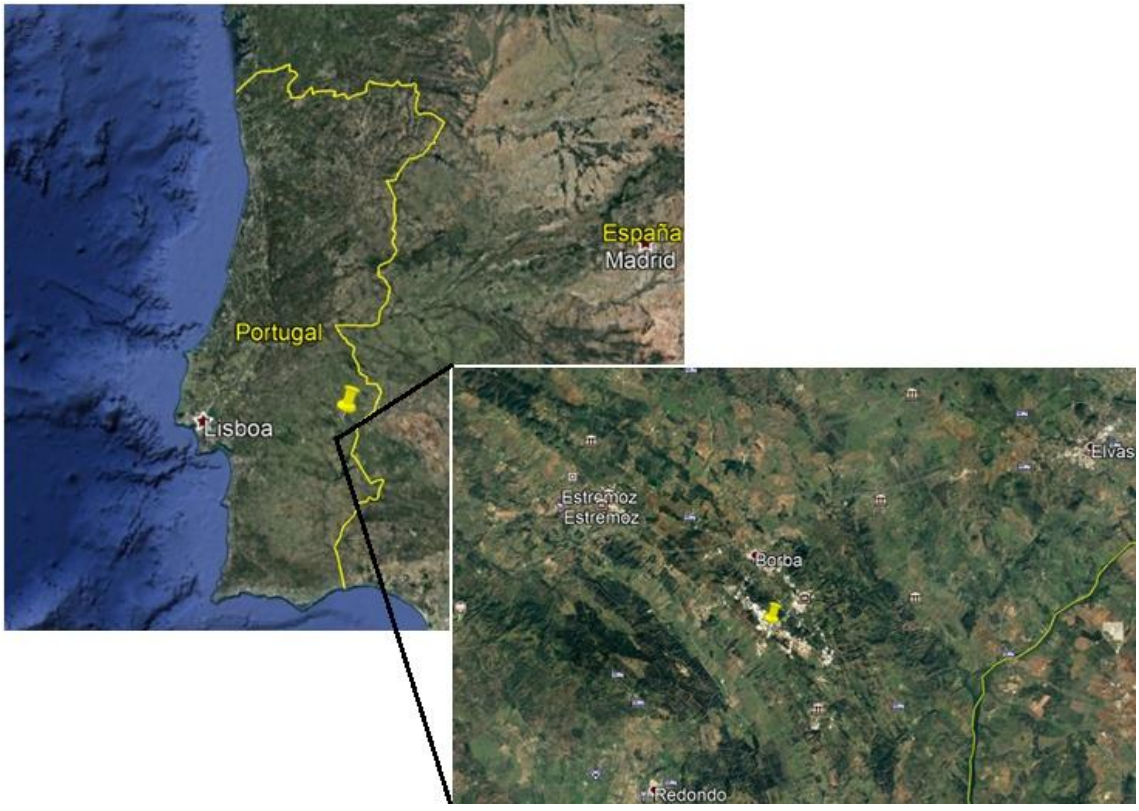

Figure 9. Location of the quarry under yellow pin. Adapted from Google Earth.

3.2. Geology

The geology where the quarry is located and by that means, the marble deposit, corresponds to a geological structure that has a grossly symmetrical shape in anticline antiform. It has an elliptical form (45x8 kilometers) that extends, according to the major axis, from the settlement of Cano, northwest, to Alandroal, southeast. It has been studied and declared that the anticline holds 100 x 106 m3 of evaluated resources and currently the exploitation covers an area of 2550 ha (Carvalho et al., 2013).

The Anticline of Estremoz - Borba - Vila Viçosa, of which the study area is part, is located in the Hercynian rockmass of the Iberian Peninsula in the Ossa Morena Zone (ZOM). The anticline is formed by rocks aged between the Upper Proterozoic and the Siluric and, in certain areas, rocks of Quaternary age, corresponding to lake deposits (Figure 10).

The geology presents a differentiation between the surface, more fractured, and deeper levels with a diachronic variation of deformation regimes. In the geological history of the Estremoz anticline, two phases of deformation are differentiated, the first one presents a compression according to the northeast - southwest direction and an important left lateral movement that is explained by the oblique convergence between the Ossa Morena Zone and the Central Iberian Zone. Then the second phase of deformation occurs, responsible for the NW-SE orientation of the Estremoz anticline and in which an accentuated segmentation in a north-northwest-south-southeast longitudinal direction occurs. These events are followed by a series of subvertical faults in a west-southwest-east-northeast direction, resulting from the traction that occurred due to the second phase of folding. The sum of west- southwest- north-east faults and the north-north-west- south-east shears is responsible for a segmentation of a block structure where, at least on the surface, the marble presents different textural characteristics. In marble, fracturing is influenced by homogeneity. So, the more homogeneous and thinner the marble the greater the chances of finding it more fractured. If this presents intercalations of pelitic rock (shale intercalations) and / or medium grain, the smaller the present fracture, due to these characteristics allowing a greater deformation when installing tensions, avoiding their rupture (Lopes, 2007).

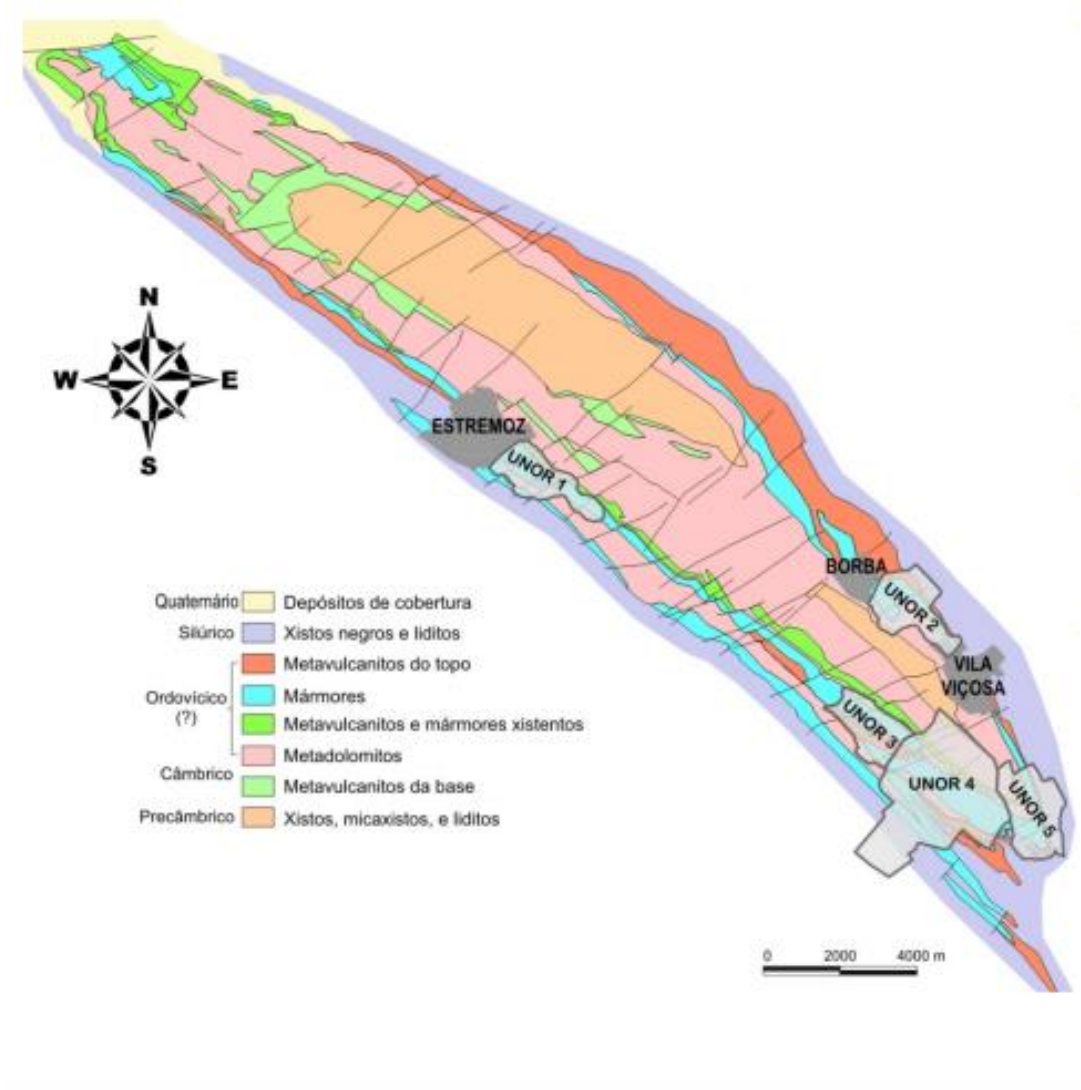

Figure 10. Estremoz anticline geology (Carvalho et al., 2010).

The lithologies involved in the mining are different-coloured marbles: blue marble, cream marble, pink marble, etc., but also primary dolomites which are locally called Cascalva rock. The marbles in the production area are at the base very bent and become purer as the stratigraphic sequence rises. The color of the marble is essentially white or cream, although for the top it may have a pinkish colour. Its thickness is about 170 metres.

The Quarry of this study is called Monte D'El Rei MJ-5282, is located in the core of quarries of Monte D'El Rei, belonging to the parish of Bencatel, in the municipality of Vila Viçosa, Évora district.

3.3. Exploitation

When designing the excavation some factors can condition, for this area, exploitability. The three most important ones are listed below.

- Fault and fracture portioning;
- Secondary dolomitization;
- Carsification.

In the first one, subdivision of the rock mass by families of faults occurs along the entire structure of Estremoz, appearing doleritic-filled veins. Its attitude is around N60ºE, vertical and the N20ºE or N80ºW, subordinate to the previous ones that can occur occasionally. Secondary dolomitization is the responsible for the transformation of marble into a secondary cavernous dolomite without ornamental aptitude (aka “olho de mocho”). And lastly, carsification, which its appearance on the exploitations is relatively frequent, especially in Borba and in some areas of Lagoa. This carsification occurs along stratigrafic planes and according to N60ºE and N10ºE direction faults. These phenomena, according to surveys conducted by the Geological and Mining Institute (IGM) they can appear up to depths of 150 m (Vintem et al., 1998).

3.3.1. Open pit Exploitation

In the Monte D’El Rei MJ-5282 quarry the extraction of material with economic value was carried out in an open pit, in depth, using the individualization technique in carved using a diamond wire. The development of extraction is descending, by benching.

The excavation of the rock mass was carried out using preparation and tracing, drilling and cutting operations, dropping, dismembering and rigging, and finally transportation of the material blocks. In order to guarantee the proper functioning of the production cycles, the exploration has a set of equipment, of which the wire machines stand out diamond drilling, deep hole drills, loaders, articulated dumpers and rotary excavators.

The top surface is 388 m.a.s.l. and the deepest surface of the pit is located at 232 m.a.s.l. which created a pit of 156 m in depth, that can be appreciated on Figure 11.

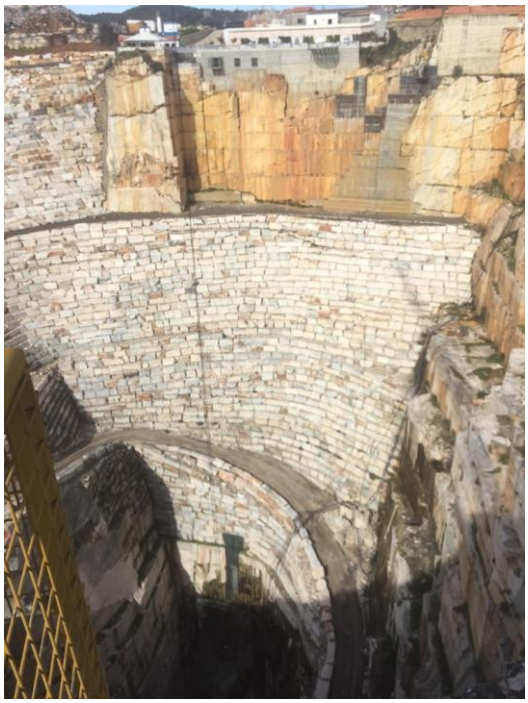

Figure 11. General view of the Northern side of Monte d'el Rei quarry.

3.3.2. Underground exploitation

After the open pit exploitation reached the limits of technology and feasibility by this method it is started to exploit via underground methods, commonly used marble quarries from top country producers (Ferrero et al., 2013). The pillar abandonment technique seems to be the most appropriate for the exploitation of this type of resource, since it allows the definition of natural support elements in the rock mass areas where the material has inferior quality, allowing, besides, to dimension the pillars in order to avoid the presence of fractures induced by the stopes. The use of this technique in quarrying may present an irregular spatial distribution of the pillars, in function of the mineral deposit heterogeneity in relation to its ornamental quality. For the Monte d'el Rei quarry, the underground exploitation is excavated from an existing open pit exploitation (Figure 12).

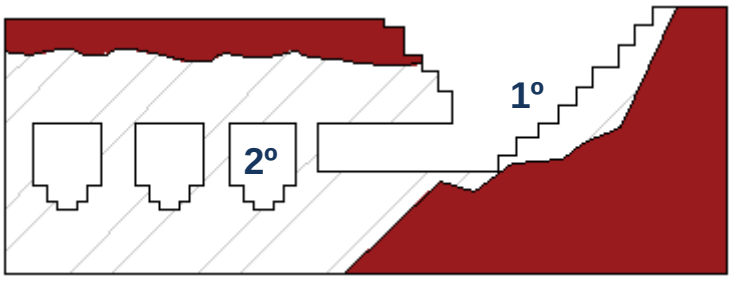

Figure 12. Mixed exploitation: 1º Open pit, 2º Drift opening from the open pit.

Rectangular galleries are the most common in the underground marble extraction industry, essentially due to rock dismantling techniques and due to the shape of the product needed (parallelepiped blocks).

At the SW end of the quarry, it can be found the opening of a semi-underground gallery, in an inverted ‘V’ shape that include the opening of a triangular section gallery at the 9th floor at 350,00 m, 5 m high and 5,7 m wide, perpendicular to the SE slope, and the development of the gallery, in 5 m recesses, maintaining the triangular geometry (Figure 13). The first lowering corresponds to the gallery's second floor (altitude 345,00 m) with a width of 11,5 m.

Figure 13. View of the inverted ‘V’-shaped semi-underground in the SW flank.(CERENA, 2019).

The quarry has mainly three accesses to the underground excavation. One being the structure explained above and two other openings, one drift being located in the interior of the dome and the other is located at the pit’s bottom level (Figure 14).

Figure 14. One of the underground openings in Monte D’El Rei quarry.

The previous figure shows the access to one of the underground openings in the SW part of Monte D’El Rei quarry.

3.4. Geomechanical characterization

The stresses acting on an underground excavation can be natural and induced. Prior to excavation in a rock mass at any point within it, there is a natural initial stress state, which is corresponding to tectonic and gravitational processes. During the underground development in the aforementioned rockmass, the final stress state depends on both the natural state and the stresses induced by the excavation.

As there is a direct relationship between the induced stresses and the initial stresses, it is obvious that the determination of the initial stress state is a condition prior to the design of any underground infrastructure.The state of natural stress or initial stress that acts on a rock mass, corresponding to in situ stress, is motivated by:

- Lithostatic stresses - due to the action of gravity also called vertical stress
- Latent stresses - of tectonic origin, effects of volcanism or contractions caused by cooling, called horizontal stresses.

When carrying out the excavation in a rock mass, there is always a redistribution of the stresses installed in the ground; this, when readjusting to the new equilibrium conditions, in a very short time compared to the geological processes, can suffer displacements that cause fracture of the rock according to discontinuity planes. The modification of the stress state contributes to the loss of strength of the material; as such, it is extremely important to assess the initial conditions to which the rock massif is subject. To analyze such stresses the triaxal shear test was carried out as presented in this chapter. Although the results give values that represent an anisotropic scenario, for the model it was taken as if isotropic. A proper determination of the state of stress in situ is needed in order to reach reliable solutions to the problem because numerical codes use stress as a possible boundary condition.

The rock mass characterization for this study has been based on laboratory mechanical tests on marble and geostructural exploration of joint sets. Numerical models of the quarry have been conceived to evaluate the behaviour of the excavation, and to relate the measured stress state of the rock mass to the numerical results. These mechanical characteristics of the rock are applied to the entire model.

3.4.1. Geo-structural characterization

Taking into account the Preliminary Study of Characterization and Assessment of Geological and Geotechnical Risks in the quarry, issued in June 2019 (Lopes et al., 2019), the characterization of the discontinuities, as it can be seen on Figure 12, was made according to the four slopes of the quarry individually, namely: Slope NW, Slope NE, Slope SE and Slope SW. For the geo-structural characterization, families of discontinuities were pointed out (Figure 15).

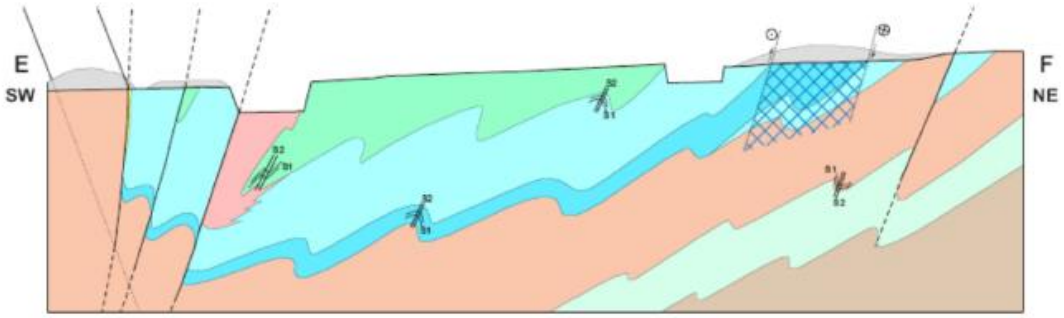

Figure 15. E(SW)-F(NE) geological section carried out in the vicinity of the study area. (LNEG, 2007).

In the characterization of the NW slope, based on observations made in 6 locations, at lower levels depth (up to about 40 m deep - elevation 350m) a shear zone with N54ºW, 80ºSW attitude, whose geomechanical quality, it is slightly altered (W1-2) and slightly fractured, sometimes moderately fractured (F2 to F3). Moreover, up to that level, three families of discontinuities were found and are represented on Table 2.

Table 2. Families of discontinuities each with its direction and dip.

Family	Direction	Dip
1	N50 - 70W	30 - 85º SW/NE
2	N10 - 30W	30 - 70º SW
3	N30 - 65E	30 - 80NW/SE

A fourth was discovered but presented a different pattern than the others, with sub-horizontal direction, it has a continuity of 3 to 10 m. All the other families have a continuity of 30 to 10 m, without apparent change. The fourth set has an opening of less than 1 mm, all other discontinuity families have an opening of 1 to 3 mm.

At greater depths, the fracturing of the rockmass in the NW slope is very reduced. Although not enough measurements have been made to quantify the fracture to date, it has been possible to identify the N20ºE, 70 º SW directions as the main discontinuities for this slope.

As regards the NE Slope, areas have been identified along approximately 20 m deep, where the rockmass is very to medium fractured, with altered rock, where the fractures openings were filled with soil. In addition, about a third of the width of the NE slope (30 m on the side left) a vertical geological fault occurs, subparallel to the doleritic vein (Cabo real - N62ºE, 85ºNW).

On the SE slope at a higher level, the same 4 families were identified on the opposite slope (NW slope) this time with higher continuity (from 10 to 30 m, with the exception of family 4 which has a continuity of 3 to 10 m) and amendment W3 to W2, according to the Basic Geotechnical Description

(BGD) classification (ISRM, 1980). In depth, it is found in development of a survey campaign that had helped to gauge the presence of discontinuities in the rockmass, despite the fact that it is self-supporting.

Finally, on the SW Slope some superficial alteration was identified in the rock as well as the main families previously identified.

3.4.2. Mechanical and physical characterization

Following the work from the Geosciences and Geoengineering Laboratory (GeoLab) of Center of Natural Resources and Environment (CERENA) at Técnico Lisboa has carried out several laboratory tests in order to determine the mechanical parameters of the rock material to sequentially start the stability studies at the exploration site.

To carry out the laboratory tests, two samples of each of the three lower levels from the exploitation, namely the levels corresponding to depths of 267 m (level 1), 246 m (level 2) and 232 (level 3). A 200 mm width cube-shaped sample was extracted (Figure 16), in order to characterize rock material directly targeted from the underground excavation.

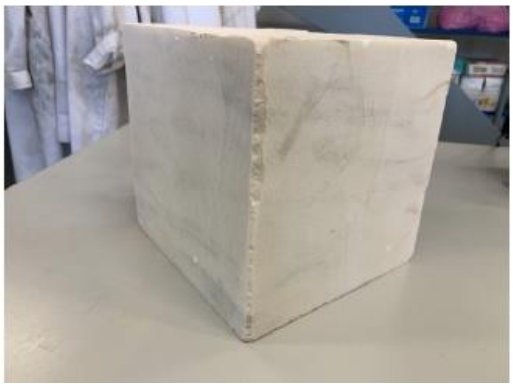

Figure 16. Sample taken from the first level. (CERENA, 2019).

The samples went under a number of laboratory tests to characterize its mechanical properties. Before tests were run, a processing and preparation of all the samples was made in strictly compliance with the requirements of the standards of the International Society for Rock Mechanics (ISRM, 2006) The set of laboratory tests comprised:

- Determination of the physical parameters;
- Determination of the indirect tensile strength (Brazilian test);
- Determination of the uniaxial compression strength with the determination of Young's modulus and Poisson's ratio;
- Determination of the triaxial compression strength;
- Determination of the direct shear strength (applied in joint samples from the three joint families).

For the first test, physical parameters such as overall density, dried and saturated density as well as porosity coefficient were calculated. Results may be seen in Table 3.

Table 3. Average values for physical properties on the three levels of samples (CERENA, 2019).

	ρ (kg/m^3)	**ρ_{seco} (kg/m^3)**	**ρ_{sat} (kg/m^3)**	**Porosity Φ**
Average value	2 687,61 ± 8,78	2 687,07 ± 8,86	2 689,89 ± 8,99	0,003 ± 0,001

In order to determine the **tensile strength**, the brazillian test was carried out (also known as diametrical compression), which is based on the application of compression forces. This method aims to determine the tensile strength without resorting to its determination by direct processes, difficult to execute in Rock Mechanics due to complicated sample preparation. The formula for calculating the tensile strength of rock is:

$$\sigma_t = \frac{2P}{\pi D h} \quad [11]$$

In the Equation 11, σ_t is the rock tensile strength (MPa), P is the specimen failure load (N), D is the cylinder specimen diameter (mm), and h is the cylinder specimen height (mm). Figure 17 shows a sample before and after the brazillian test.

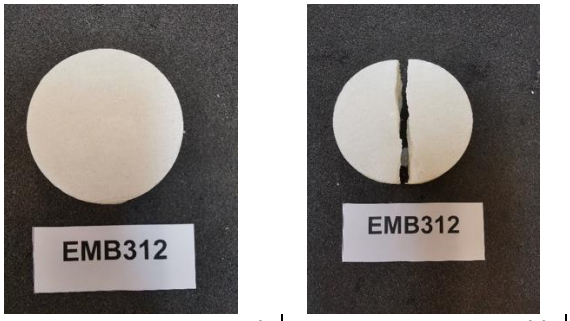

Figure 17. Sample from level 3 before a) and after b) the brazillian test (CERENA, 2019).

For the **uniaxial compression tests** it is aimed to determine the longitudinal and transverse strain of the specimen under unconfined and uniaxial compressive stress and calculate the rock compressive strength, elastic modulus, and Poisson's ratio. The determination of the maximum stress value (σ_c) is calculated from the record of the maximum load, when the specimen it is forced uniaxially until failure. Taking into account the suggestions from (ISRM, 1979), 53 mm diameter specimens were prepared, whose ratio height / diameter was 2,5 (Figure 18)

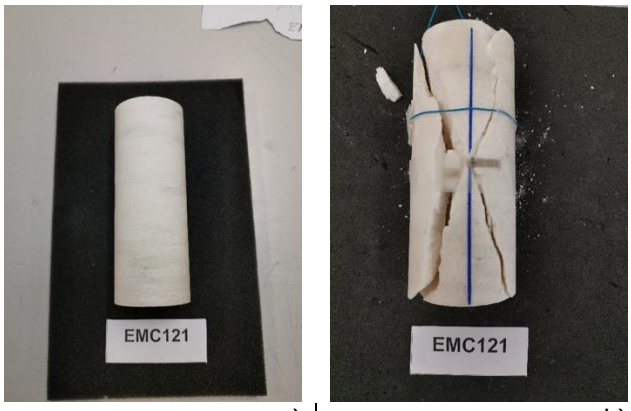

Figure 18. Sample from level 1 before a) and after b) the uniaxial compressive strength test (CERENA, 2019).

Specimens strain was obtained by strain gauges that were installed directly in the samples lateral surface.

The formula for calculating the average elastic modulus E_{av} is (ISRM, 1979):

$$E_{av} = \frac{\sigma_b - \sigma_a}{\varepsilon_{lb} - \varepsilon_{la}} \quad [12]$$

In equation 12, σ_a is the stress value of the beginning point of the linear segment on the stress-strain relation curve (MPa); σ_b is the stress value of the end of the linear segment on the stress-strain relation curve (MPa); ε_{la} is the axial strain value when the stress is σ_a, and ε_{lb} is the axial strain value when the stress is σ_b .

And for the Poisson's ratio the formula is (ISRM, 1979):

$$\mu_{av} = \frac{\varepsilon_{db} - \varepsilon_{da}}{\varepsilon_{lb} - \varepsilon_{la}} \quad [13]$$

In equation 13 μ_{av} is the average Poisson's ratio of the rock, ε_{la} is the axial strain value corresponding to the previous σ_a. ε_{lb} is the axial strain value corresponding to the previous σ_b. ε_{da} is the radial strain values corresponding to the previous σ_a. ε_{db} is the radial strain values corresponding to the previous σ_b (ISRM, 1979) .

In Table 4 tension strength values and uniaxial compressive values for samples of the three levels. EMC1xx corresponds to the first level; EMC2xx to the second level and EMC3xx to the third level. Regarding the tests to determine the resistance to uniaxial compression, any abnormal values were recorded for all determined parameters (σc, E and υ).

Table 4. UCS test values for each sample for each level (CERENA, 2019).

Sample	Uniaxial compressive strength	Young's Module E	Poisson's coefficient v
EMC111	75,57	62,28	0,26
EMC112	67,57	64,26	0,23
EMC121	77,41	58,52	0,24
EMC122	75,79	51,32	0,25
EMC211	57,35	62,38	0,24
EMC212	66,44	65,15	0,27
EMC221	64,83	60,64	0,22
EMC222	74,48	57,14	0,26
EMC311	65,82	50,35	0,22
EMC312	67,3	58,33	0,26
EMC321	67,57	50,36	0,22
EMC322	68,93	50,67	0,24

For the **triaxial compression test** the test pieces, 42 mm in diameter and a height / diameter ratio of 2, (Figure 19) follow the specifications recommended in the ISRM Suggestion Methods (ISRM, 1978), on which a triaxial Hoek Cell was used (Figure 20). A cylindrical specimen is required and is first subjected to lateral pressure and then deviator stress.

In the usual procedure, the specimen is subjected to confining pressure (p) and then deviatoric stress is applied when the confining pressure is kept constant. The confining pressure P increases the strength of rock. However, the increase in strength is realized only when the specimen is immersed in impervious jacket. Generally hydraulic oil is used as confining fluid and the jacket is made of polyurethane which is oil resistant.

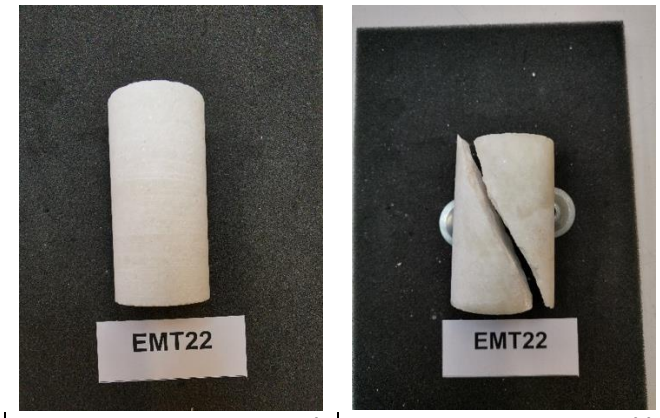

Figure 19.Sample from level 2 before a) and after b) the triaxial compressive strength test (CERENA, 2019).

Figure 20. Hoek Cell.

The triaxial compression strength (σ_1) is calculated by dividing the maximum axial load applied to the specimen, for a given confining pressure (σ_3). It was thus possible to apply three different levels of confinement pressure of 2, 4 and 6 MPa. As it turns out, for the highest levels of confinement pressure, it is obtained higher values to triaxial compression strength (Table 5).

Table 5. Result extraction from laboratory tests on triaxial compression (CERENA, 2019).

Sample	σ_3 (MPa)	σ_1 (MPa)
11	2,00	58,16
12	4,00	99,37
21	6,00	85,58
22	4,00	83,87
31	6,00	96,99
32	2,00	70,93

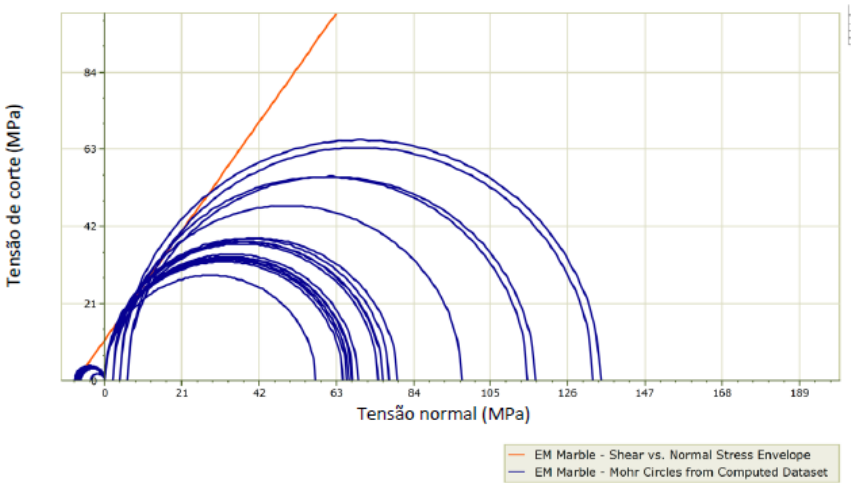

Figure 21. Mohr circles and Mohr envelope for the tests results. (CERENA, 2019).

Finally, taking into account the results of the tests for determining the tension strength, uniaxial compression and triaxial compression, it will be possible to trace the respective Mohr circles and, by applying a linear adjustment, the respective Mohr-Coulomb envelope as seen in Figure 21.

Hence, the cohesion values and the friction angle of the tested marble material are determined. 11.15 MPa and 54.67º, that appear in Table 6 along with a summary of the average values of each parameter determined through the tests explained above.

Table 6. Average values from the strength and elastic parameters (adapted from: CERENA, 2019).

	Tensile strength σ_t (MPa)	**Compressive strength σ_c (MPa)**	**Elastic module E (GPa)**	**Poisson's ratio υ**	**Cohesion *c* (MPa)**	**Internal friction angle φ (º)**
Average value	7,31 ± 0,56	69,09 ± 5,77	57,62 ± 5,64	0,24 ± 0,02	11,15	54,67º

As for the test on **direct shear strength over discontinuities** from the different joint families, the method was carried out in a laboratory as well (Figure 22), differing from the in situ shear strength one. This test measures peak and residual direct shear strength as a function of stress normal to the sheared plane (Muralha et al., 2014) The aim of the shear strength of rock discontinuities is essential for stability studies and requires the determination of important frictional parameters as well as the quantification of the influence of factors such as surface roughness, impersistence and infill for the discontinuity in situ.

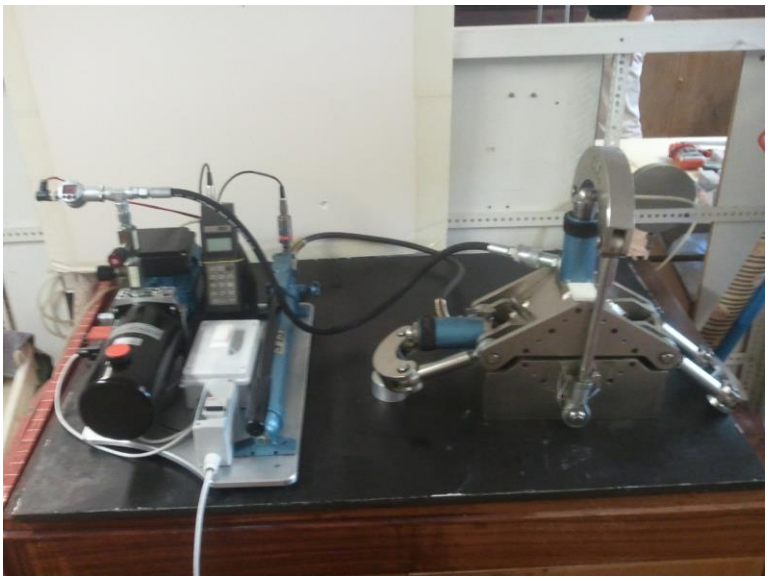

Figure 22. Direct shear strength apparatus at GeoLab/CERENA.

The procedure of the test begins with a preparation phase where the sample is dimensioned and encapsulated followed by a consolidation stage, where the specimen is places into the shear box and all the gauges have been set. First readings of displacement can be read in this phase. Lastly,

shear loading is applied and measures can be taken. Peak and residual strength are obtained from the calculations and plotting them against a normal stress graph, friction angle and cohesion values can be extracted. From the test made on the three different discontinuities of the area, Table 7 summarizes the obtained results.

Table 7. Results from the shear strength test on the three discontinuity families (CERENA, 2020).

Families of discontinuities	c (MPa)	Φ (º)
Family 1 (N60ºE)	0,14	42,04
Family 2 (N20ºW, 72ºS)	0,25	46,05
Family 3 (N40ºW, 72ºN)	0,31	51,32

From these test, strength and elastic values are retrieved for the further geomechanical characterization of the model. It is worth mentioning that in all the three levels, no particular or strong differences in values were found when doing the laboratory works.

4. Methodology

4.1. Room and pillar design

Using the room and pillar method, the material is extracted by horizontal or sub-horizontal excavation, advancing along multiple operating fronts leaving chambers separated by pillars. The result is usually a regular layout of stopes and pillars with a size that depends on the stability and thickness of the deposit, but with the aim of extracting as much material as possible.

Pillars are required to both offer global stability, to support the overlying strata, and local stability, which is defined as stable ribs and roof spans between the pillars, and that is required to provide safe working conditions. Pillar design is typically carried out by estimating the pillar strength and the pillar stress, and then sizing the pillars so that an adequate margin exists between the expected pillar strength and stress. When designing a system of pillars, the FS is critical to stability, because it must compensate for the variability and uncertainty related to pillar strength and stress and varying dimensions of rooms and pillars.

These pillars may be partially or fully recovered at the end of the exploitation. This requires an exhaustive study of factors such as pillars or roof layers strength. The chambers between the pillars serve as a passage for the trucks that transport the material to the mine's stockpile. The exploitation is carried out gradually from the top, allowing the roof to be secured at an appropriate height for the equipment.

According to the (US Bureau of Reclamation Engineering, 1977) the safety factor depends on the quantity and quality of information used to estimate the loads and strength of the rock. This factor is the resistance/strength ratio, which must always be greater than the unit in order to have stable pillars, i.e. the resistance of the pillars must always be greater than the acting stress. If the information on the rock mass quality and the geology is thoroughly studied the safety factor is around 2-3. If above that laboratory test are run, the safety factor can go down to 1,5-2. The safety factor goes by the Equation 14:

$$FS = \frac{Pillar\ strength}{Actual\ pillar\ stress} = \frac{S_p}{\sigma_p} \qquad [14]$$

Defining the safety factor is a basic step to define the stability of the excavation.

One of the ways to estimate the stresses in pillars is by the application of the tributary area theory that assumes that a pillar will be supported if it shares the applied load (Bunting, 1911). This theory is applicable to situations where similar pillar shapes are developed in large regular areas (Figure 23).

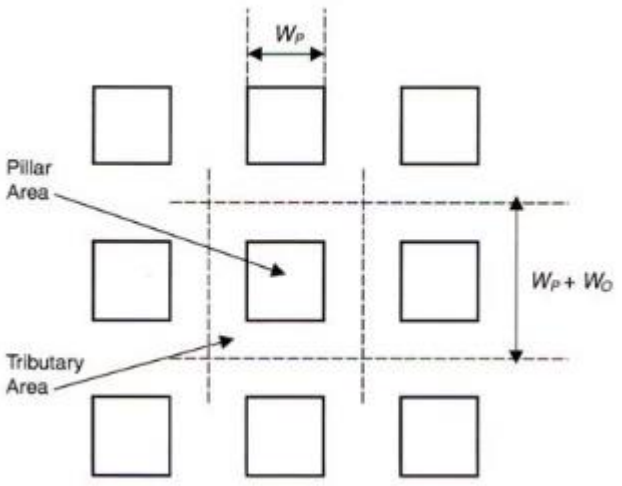

Figure 23. Tributary area method sketch (Brady & Brown, 2006).

In Figure 23, W_p is the pillar width and W_o is the width of the chamber. The picture above follows the next equation, [15], when calculating the pillar stress, σ_p, for square pillars (Brady & Brown, 2006):

$$\sigma_p = \sigma_z * \left[\frac{W_p + W_o}{W_p}\right]^2 \qquad [15]$$

Where σ_z is the vertical stress [16], due to the action of gravity, that is determined by the depth (m) at which the mineral deposit is located and the specific weight of the material (γ):

$$\sigma_z = \gamma * Z \qquad [16]$$

Other types of pillars may present, rectangular shapes [17] (Figure 24):

$$\sigma_p = \sigma_z * \left(\frac{W_p+W_o}{W_p}\right) * \left(\frac{1+L_o}{L_p}\right) \quad [17]$$

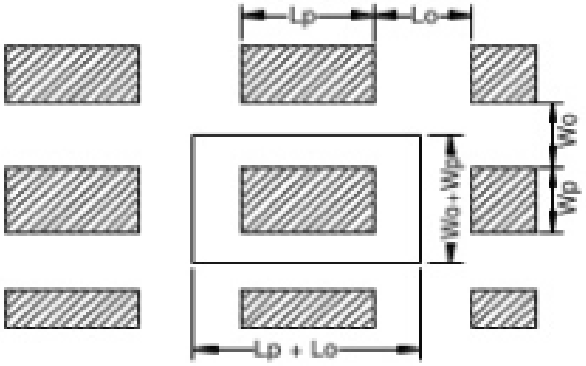

Figure 24. Tributary area method sketch for rectangular pillars (Brady & Brown, 2006).

As well as for rib pillars [18] (Figure 25):

$$\sigma_p = \sigma_z * \left(1 + \frac{W_o}{W_p}\right) \ (MPa) \quad [18]$$

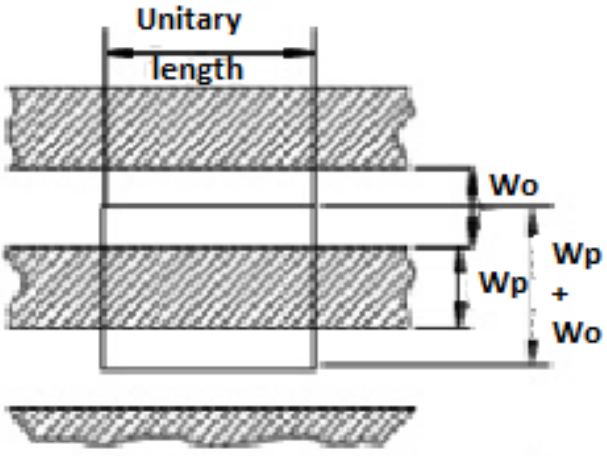

Figure 25. Tributary area method sketch for rib pillars (Brady & Brown, 2006).

Next, it is necessary to calculate the strength of the pillar. Based on extensive observations of pillar behaviour in mines, many authors such as Lunder & Pakalnis (1997), Hedley & Grant (1972), Salamon & Munro (1967) and Duvall (1976) have come with several ways to estimate the pillar strength. Salamon & Munro (1967) presented the most used formula [19] for coal pillars to estimate pillar strength by:

$$S = K * \frac{W^{\alpha}}{H^{\beta}} \quad [19]$$

Where W is the width of the pillar, H is the height of the pillar, K is a parameter related to the rock strength (UCS) and α and β are parameters related to the geomechanical conditions of the rock mass.

Esterhuizen et al. (2008) with previous knowledge of Roberts et al. (2007), presented a formula to estimate pillar strength that is more appropriate when mining natural stone. This formula derives from the Salamon & Munro (1967) equation but with specific coefficients calculated through the study of several underground quarries throughout United States. This equation [20] can be used to estimate the average strength of pillars in flat-lying room-and-pillar stone mines. The equation specifically excludes cases where the floor may yield or low strength bedding bands exist that can extrude and weaken the pillars.

$$S = k * \frac{W^{0,3}}{H^{0,59}} \quad [20]$$

With k being [21]:

$$k = 0{,}65\ x\ UCS \quad [21]$$

And the Uniaxial Compressive Strength (UCS), will be retrieved for the calculation above, from the laboratory test, where it measured an average value of 69,09 MPa.

For the recovery equation [22] it will be used the following:

$$e = \frac{At-Ap}{At} = 1 - \frac{WpLp}{(Wp+Wo)(Lp+Lo)} \quad [22]$$

In which At represents the total area or tributary area; Ap represents the pillar area; Wp expresses the pillar width; Lp expresses pillar length and (Wp+Wo) and (Lp+Lo) the width and the length of the total area (Palma Guerreiro, 2000).

Retrieving from Esterhuizen et al. (2008), the study shows that a minimum of 1,2 m thick crown pillar is necessary to ensure roof stability. For this study the beam thickness will be round up to 2 m, in sake of safety. To determine the depth of confinement, the net value of the open pit depth, from the surface to the lowest point excavated in the pit, 156 m, it will be added to this beam thickness, 2 m. This gives a confinement depth of 158 m (Z).

For this depth is going to be considered three types of room and pillar dimensions, taking recommendations from previous literature on room and pillar stone mining, so when applying the Tributary Area method, the safety factor and recovery of each scenario can be discussed.

Knowing from the laboratory tests that specific weight is 26,88 kN/m^3 or 0,026 MN/m^3, the vertical stress is [23]:

$$\sigma_z = \gamma * Z\ = 0{,}026 * 158 = 4{,}11\ MPa \quad [23]$$

And also for the parameter k [24], related to the rock strength:

$$k = 0{,}65\ x\ 69{,}09 = 44{,}9\ MPa \qquad [24]$$

Large discontinuities should only be considered for the design when pillars are intersected by them, according to Esterhuizen et al., 2008. From the same paper it can be draw that discontinuities can have a significant impact on pillar strength and the impact is exacerbated as the width-to-height ratio decreases. To asses discontinuities of pillars, the authors suggests using Discontinuity Dip Factors (DDF). However, these factors would be conservative for assessing a layout of many pillars, because the large discontinuities can be widely spaced and may not necessarily intersect every pillar. Large Discontinuity Factors with Frequency Factors will be more applicable for this case, but in order to consider them a detailed 3D layout with discontinuities should be available.

In the table below, Table 8, it was also calculated the width to height ratio in order to confirm stability for the dimensioning, as the ratio has to be higher than 1 to be considered stable. Although this is an important calculation it does not ensure local stability for the pillar, many other factors go with it, as explained in previous chapters.

Table 8. Possible scenarios for the depth given with room and pillar characteristics.

Z=158 m	A	B	C
Pillar width W (m)	10	15	18
Pillar height H (m)	7,5	7,5	7,5
Width to height ratio	1,3	2,0	2,4
Room width B (m)	10	14	17
Pillar strength σ_r (MPa)	27,29	30,82	32,56
Actual pillar stress σ_p (MPa)	16,43	15,35	15,53
Safety factor FS	1,66	2,01	2,10
Recovery %	75%	73%	74%

To optimize the recovery and taking into account the safety factor typically used for such marble stone quarries (S.F. = 1,2) pillar strength and actual pillar stress need to be calculated with the formulae explained above (Esterhuizen et al., 2008). All safety factors (A, B and C) are higher than the recommended from literature, so taking into account that scenario A gives the higher recovery

percentage, option A will define the dimensions of the room and pillar excavation for this study. It will be a square pillar (10x10 m) with a height of 7,5 m.

Next step will be to design the layout for the excavation and for this, the drafting software AutoCad will be used. Firstly the previously design model of the quarry, will be examined and knowing the limits of the exploitation license, a square area within it is going to be draw in order to create a simpler area to study. Secondly, square pillars will fill this area given the dimensions above.

4.2. Geomechanical analysis

In order to carry out the geomechanical analysis through a numerical model the Finite Element Method software RocScience Inc in 3D – *RS3*, was used. *RS3* (R stands for Rock and S for Soil 3 for three dimensional analysis) is a 3D FEM tool from Rocscience Inc for analysis of geotechnical structures for civil and mining applications. It can be used for a wide range of applications from tunnelling and support design, surface excavation, embankments, and foundation design and seepage analysis (Sarathchandran, 2014). It allows to simulate the behavior of the rock mass in the vicinity of the excavation and to evaluate the safety of the exploration through the study of the geomechanical behavior and the rock mass stability conditions. To perform a useful numerical analysis a geotechnical engineer requires a knowledge in a broad range of subject as well as being conversant with finite element procedure, concepts of rock mechanics and more importantly the knowledge of constitutive models and solution algorithms used to implement it.

A geomechanical model is a tool that allows the reproduction, with the greatest possible realism, of the characteristics and reactions of a rock mass, simulating its behavior when applying external stresses, for example, the opening of a cavity inherent to an underground exploration.

4.2.1. Excavation geometry

Imported from the AutoCad design (*Figure 26*), the geometric definition of the model consisted of the reproduction, at the real scale, of the reality existing in the exploration in order to simulate the rock mass response with the greatest reliability.

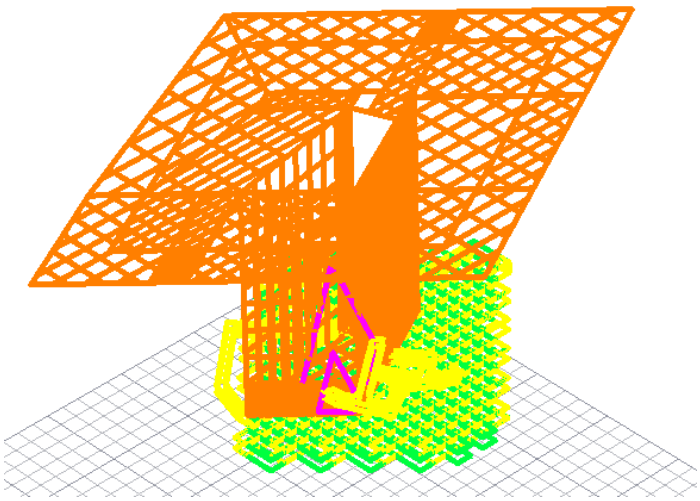

Figure 26 . Representation in Autocad of the quarry.

The excavation was defined by an excavation limit and filled up with the previously designed pillars, in total this area has 36 640,41 m^2 and a perimeter of 775,3 m, which allows a total number of 80 pillars. In this excavation all pillars will be considered squared pillars.

The rest of the model belongs to previous works on the quarry and consist on a simplified model but still being representative enough. The model is divided given the type of function/representation of the quarry. Firstly there are the geometries created to represent the open pit and the surface, secondly there are the preexisting excavations, these being the drifts that connect the underground excavations with the open pit exploitation. There is also a representation of the inverted v-shape structure the domed access in the southeast flank. When creating the excavations from the room and pillar layout, features from RS3, Rocscience will be used. Those tools, among others, were used to create primitive boxes. In Figure 26, these primitive boxes will be the green and yellow prisms that will cut each other and with the option from RS3, Substract, it will be possible to create pillars, that will be given an applied property of 'No Material' or 'Material', depending of its applied function, so the software recognizes it as a structure within the model scope.

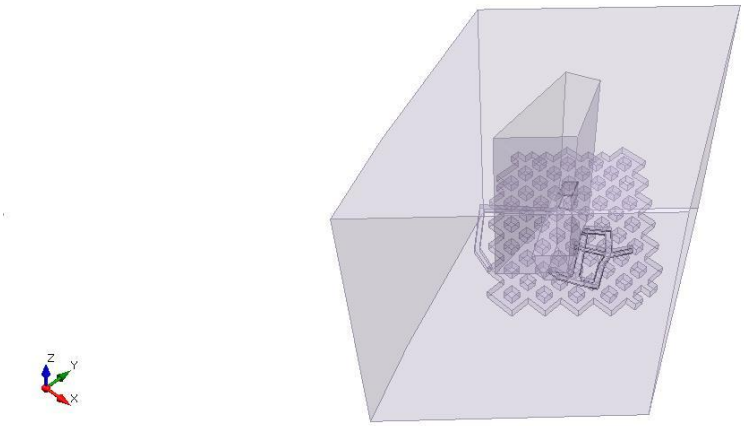

Figure 27. Representation of the external volume and the excavation.

Translating the AutoCad model to RS3, this is the final look when creating the geometry (*Figure 27*). The lower level where the excavation takes place will be connected to the surface through an access ramp developed from a preexisting drift. Through said ramp, mining operations in the room and pillar area, such as hauling will be done.

4.2.2. Geomechanical characteristics

For the model it was assumed that the rockmass was isotropic, linear and elastic. In order to make it more realistic when choosing the yield criterion the jointed Mohr-Coulomb version was defined, as explained, in the geo-structural characterization the quarry is crossed by three families of discontinuities. For the mechanical parameters of the rock the average values obtained from the geomechanical characterization was considered (Table 9).

Table 9. Properties for marble considered in the model.

Material	**Tensile strength, σt (MPa)**	**Young's module, E (GPa)**	**Poisson's ratio, υ**	**Cohesion, c (MPa)**	**Internal friction angle, φ (º)**
Marble	7,31	57,62	0,24	11,15	54,67 º

To complete rock mass modelling, the joint characteristics, needed to apply when assigning material properties for marble, taken from the direct shear strength test, which properties are summarized in Table 10.

Table 10. Defining properties for the three families of discontinuities on RS3.

	Joint 1	**Joint 2**	**Joint 3**
Peak cohesion (MPa)	0,14	0,25	0,31
Peak friction angle (deg)	42,04	46,05	51,32
Trend (º)	60	20	40
Plunge (º)	90	-72	72

As for the rockfill modelling, the developed model considers the consolidated cemented rockfill properties, following the Mohr-Coulomb failure criterion, as stated by Warren et al. (2018) and Shresta et. Al (2008). Those properties are presented in Table 11.

Table 11.Properties for cemented rockfill.

Material	Tensile strength σ_t (MPa)*	Elastic module E (GPa)**	Poisson's ratio υ**	Cohesion c (MPa)**	Internal friction angle ϕ (º)**
Cemented Rockfill	3,17	3,5	0,3	1,5	40

* Warren et al., 2018,** Shrestha et al., 2008

Note for the fact that the developed model does not considers the influence of water.

4.2.3. Boundary conditions and Restrains

Boundary conditions are a stated restriction, usually in the form of an equation that limits the possible solutions to a differential equation. When all excavation structures are modeled, boundary conditions need to be defined so as the program executes the simulation in a closed scope. For this, the maximum area of the surface that covers the whole model will be extruded in a depth that the application of boundary conditions does not affect the results and following, this volume will be set as External, which is the RS3 feature to define said conditions. In statics, their role is played by restraints and external loads applied to the system. As for the restrains, RS3 will provide with comfortable tools to define restrains in every axis direction. This process will fix the model in space in order to satisfy the force balancing that the Finite Element Analysis requires.

4.2.4. Meshing

As for the mesh operations a 10-noded tetrahedra graded mesh was considered so result values were more precise. The finite elements are constructed from the union of these points, in this case three to three (since the mesh is triangular) obtaining a regular mesh that allows the treatment of the rock mass as a continuous medium Because of the model extension, grid size was too large to be applied to every part of the model, so two grid refinements were done, specifically in the room and pillar excavation and in the dome structure. The finite-element mesh contained 44 047 elements with 60 908 nodes (*Figure 28*).

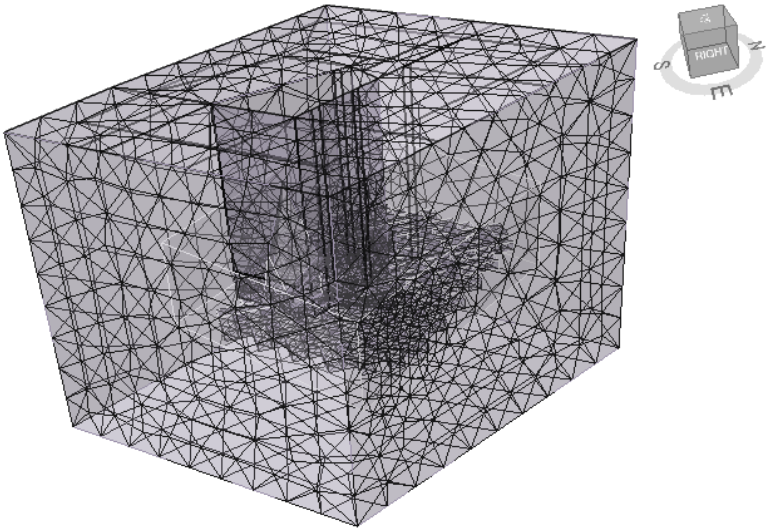

Figure 28. Finite Element mesh for the quarry model.

4.3. Rock Backfill Recovery Method

The process will start with the waste material from the quarry being processed in a plant. That plant is composed by basic equipment so its construction nearby the quarry will not only be convenient and cost saving, but rather simple. In this plant the mixture of aggregates and additives will be made previous to its combination with cement which will be performed already in the underground excavation to maximize the mixture and the setting times. The resulting backfill will be transported through filling pipes to the mined room for its filling. The suggested process follows the one given by Zou *et al* (2019) on the Ershike coal mine, located in Hengshan County, Yulin City, Shaanxi Province in China (*Figure 29*). Even though this study takes into account parameters such as solidification time and the mine's periodic weighting, for this own study it will be focused more on the layout of backfilling itself for later numerical estimation of stability, so for that, mechanical parameters such as strength parameters and elastic parameters will be taken as if already consolidated. It will be also considered a tightfill situation (Murch, 2018), i.e. all volumes will be backfilled up to its totality, so convergence from the drift ceiling is avoided. Actually, there are several issues concerning with the complete or incomplete benchfilling, which are not in the aim of the present work.(Bloss, 2014; Rodrigues et al., 1993; Haixiang, 1999).

In essence, the recovery of residual pillars via rockfilling is the use of the support given by a rock-filled structure instead of the residual marble pillars.

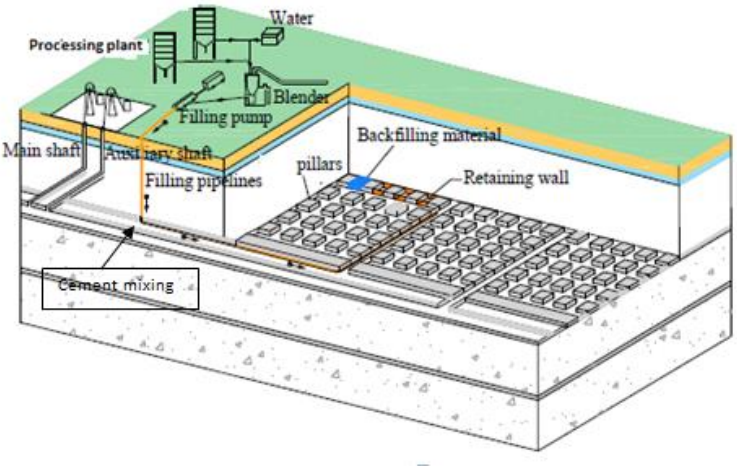

Figure 29. Backfill operations and cement distribution into the excavation.(Zhou et al., 2019).

Due to rock-filled structures can withstand the load of overburdened rock, it effectively shares the supporting strength of the residual pillars and is therefore capable of achieving partial or total recovery of the residual pillars room.

In the developed model, the excavation layout will be divided into areas so operations can be safely carried out and will start from the furthest point of the working face. A retaining wall will be constructed between two pillars to create an enclosed structure, in sets of columns, leaving a pillar volume space between backfilled pillars. With pipelines, CRF will be laid in that enclosed volume and create the new CRF pillar. The areas selected in this study are three different layouts (Figure 30) that progressively face the only access to the excavation, the ramp, where loading and hauling operations will occur.

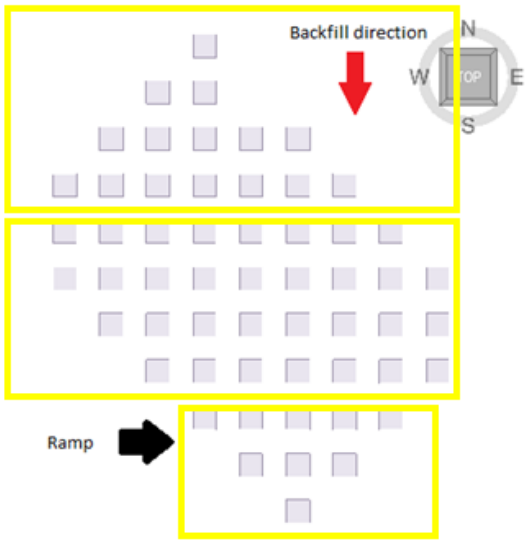

Figure 30. First layout of the room and pillar excavation backfill direction (N-S), ramp access and the three operation areas.

Table 12. Backfill and pillar removal sequence in the three areas.

Stage	Description	Area 1	Area 2	Area 3
1	Excavation	excavated	excavated	excavated
2	BF*1	1st backfill	excavated	excavated
3	BF2	pillar removal	excavated	excavated
4	BF 3	2nd backfill	excavated	excavated
5	BF 4	---	1st backfill	excavated
6	BF 5	---	pillar removal	excavated
7	BF 6	---	2nd backfill	excavated
8	BF 7	---	---	1st backfill
9	BF 8	---	---	pillar removal
10	BF 9	Total backfill	Total backfill	Total backfill

**BF: Backfill*

In the RS3 model, this sequence of excavation and backfill has set 10 different stages (Table 12). The first, called 'Excavation' will consider the quarry and the underground openings as it had already been excavated, following, the next 9 stages are all about backfilling the room and pillar drifts and removing the residual pillars until stage 10 where all the considered area is backfilled completely. Taking from Zhou et al. (2019), the backfill and the sectioning proposal, in this study the first area will cover a total of 16 residual pillars going in a north-south direction. Chambers will be filled every two pillars. The operations will start with the creation of new pillars (Figure 31 left picture) around the residual ones, followed by the removal of the latter ones (Figure 31 right picture) and concluded with the backfill of the excavated space created when removing the marble pillars (Figure 32 left picture). For such sequence, area-length drifts will remain excavated until the last stage, to allow hauling and loading operations, where ultimately they will be also backfilled for higher support.

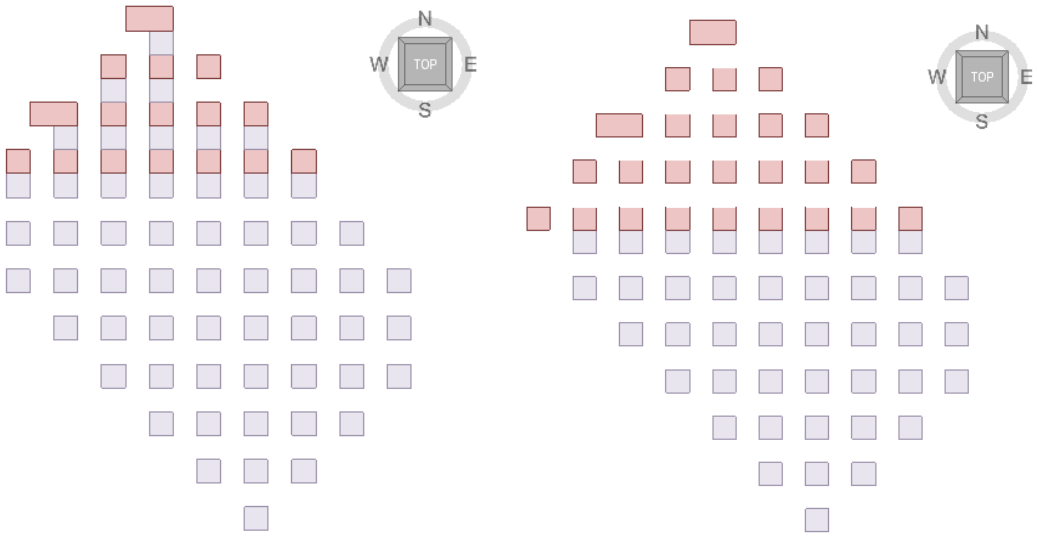

Figure 31. Backfill of W-E columns of pillars BF1 (left) and removal of residual pillars BF2 (right). Residual pillars are on grey and backfill pillars on pink colour.

For the first area a total of 16 pillars will be backfilled and let to set and dry for 3 days (Neville, 2009). Already in the third stage of the project it will be first proceed to remove residual pillars from the first area (*Figure 31*), 15 residual pillars will be recovered.

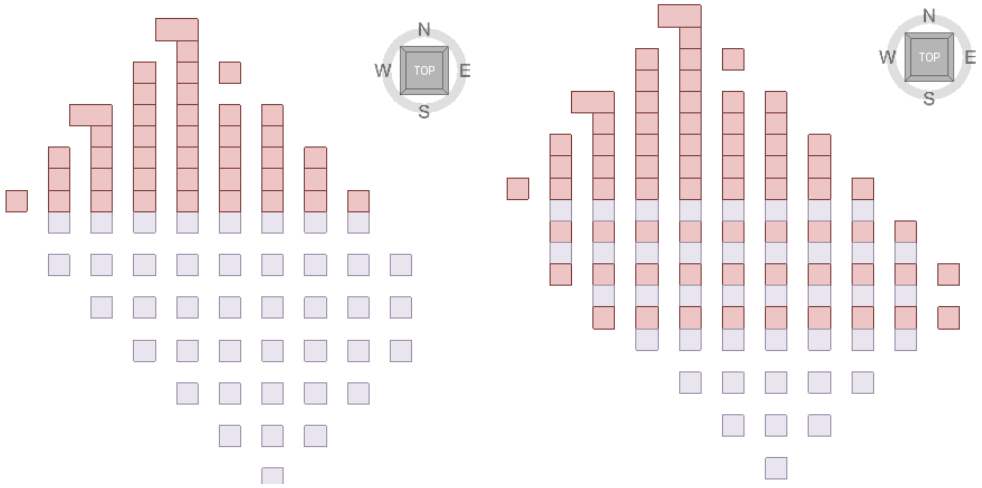

Figure 32. Backfill of the residual pillar's spaces BF3 (left) and backfill of the next area's W-E columns of pillars BF4 (right). Residual pillars are on grey and backfill pillars on pink colour.

In addition to the pillar removal, the volumes left by this operation will be backfilled as well to maximize safety conditions (*Figure 32* right picture). Secondly, the second area (*Figure 33*), and 5th stage will be treated with the same procedure as before, this is, first creating support rockfill pillars, secondly, the removal of residual pillars and thirdly, the backfill of the openings left behind, with the exception of the N-S drifts that will be backfilled in the last stage to ensure until then mining operations.

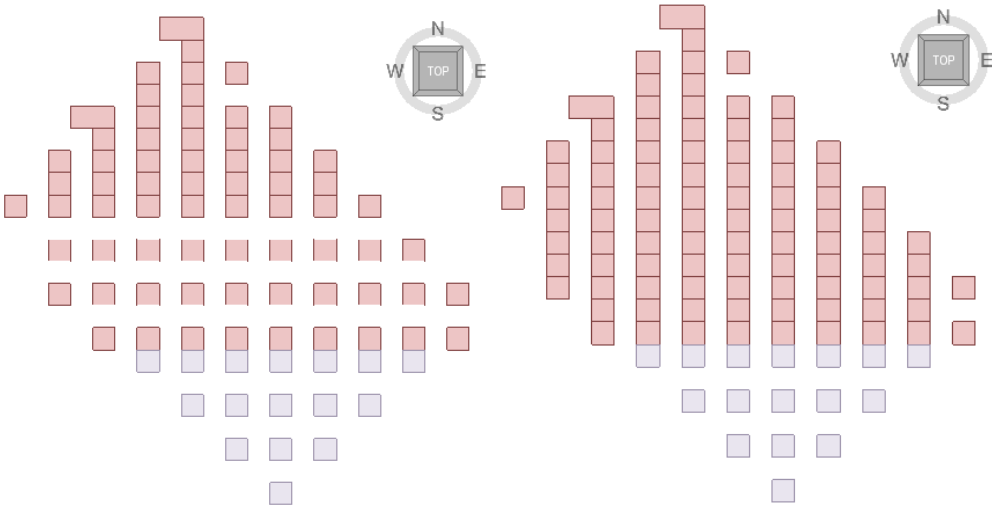

Figure 33. Removal of residual pillars BF5 (left) and backfill of the spaces created BF6 (right). Residual pillars are on grey and backfill pillars on pink colour.

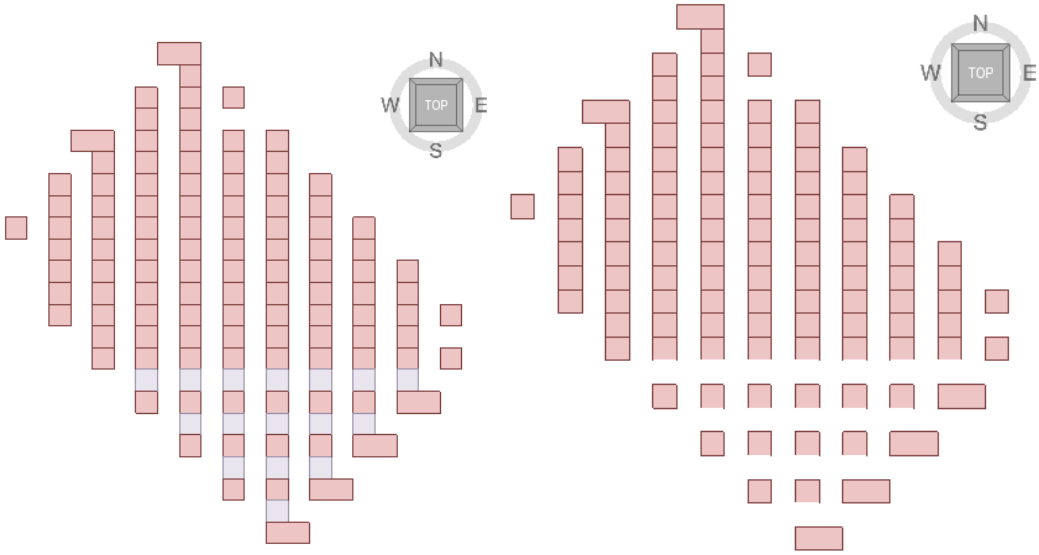

Figure 34. Backfill of the last area of the excavation BF7 (left) and removal BF8 (right). Residual pillars are on grey and backfill pillars on pink colour.

In Figure 34, the last area of the excavation is treated in the same way as the two before, just with a difference that is, when backfilling the spaces left from the removal of the residual marble pillars, north-to-south drifts will be also backfill (*Figure 35*), completing in this way all open underground spaces. From this operation a total of 56 pillars will be recovered.

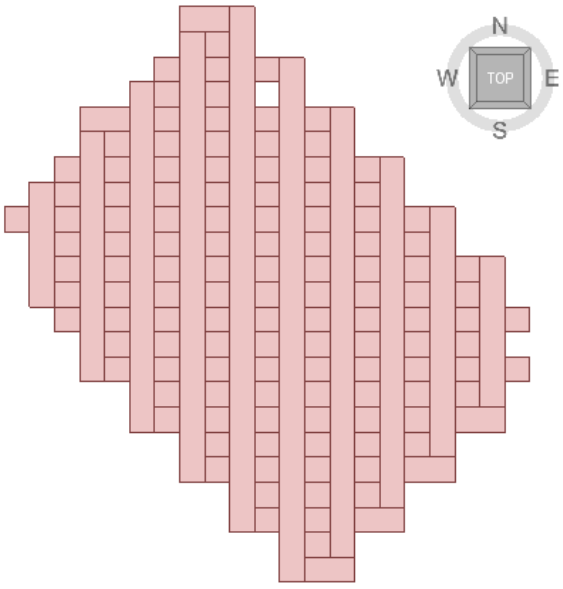

Figure 35. Complete backfill BF9 (N-S drifts included).

Knowing the steps of the methodology and how it is going to be approached the backfill sequence, it is only time to read results and make assumptions on the computed model.

5. Interpretation of Results

In this chapter results for the simulation explained above are presented and commented with the help of graphical representations and pictures of the results as seen as in the results tab in the software RS3.

5.1. Strength Factor

When analyzing results from a numerical computation in order to characterize stability, one of the first data group that should be looked into is the strength factor. The strength factor is calculated by dividing the rock strength by the induced stress at every point in the mesh [25]. All three principal stresses have an influence on the strength factor (Sigma 1, Sigma 2 and Sigma 3). In the case of elastic materials, the strength factor can be less than unity, since overstressing is allowed. In the case of plastic materials, the strength factor is always greater than or equal to unity. (Rocscience Inc, n.d.). As in this study it was chosen the Mohr Coulomb yield criterion, used to describe the real rock stress-strain response with an idealized elastic-perfectly plastic stress strain curve. Hence, values from the result tab on the strength factor parameter can indeed go below 0 (Rocscience Inc, n.d.).

$$Strength\ factor = \frac{Rock\ strength}{induced\ stress} \qquad [25]$$

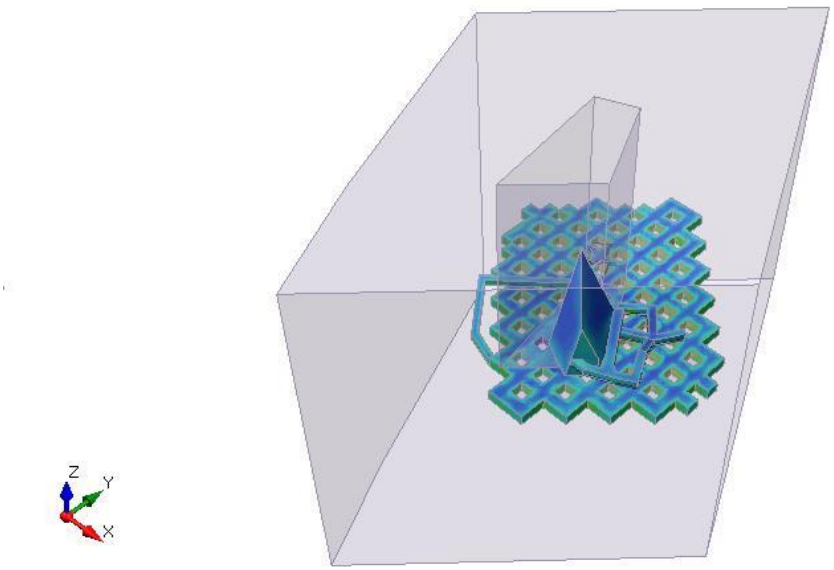

Figure 36. Representation of the excavation on its initial phase (Excavation).

When looking for weaker spots in the excavation, isosurfaces of a certain desired strength factor value were created. The first isosurface had a value near to 1, but slightly below 0,9, so unstable areas can be studied for other parameters along all the stages. For the first stage, this is the excavation stage, where drifts are already created, no areas with a strength factor below one are spotted, this proves that for an initial stage where a room and pillar excavation is excavated, Figure 36, it will remain stable. This situation, where the strength factor is higher or equal to one, appears

also for stage 2, where backfilling of cubic pillars around the vertical axis of the residual pillars happens (Figure 30 left), but no residual pillars are removed yet. Only in stage 3 (BF2), is when a strength factor of 0,9 starts to show. This can be explained due to the removal of the pillars and the support solely done by one set of backfilled pillars (*Figure 37*).

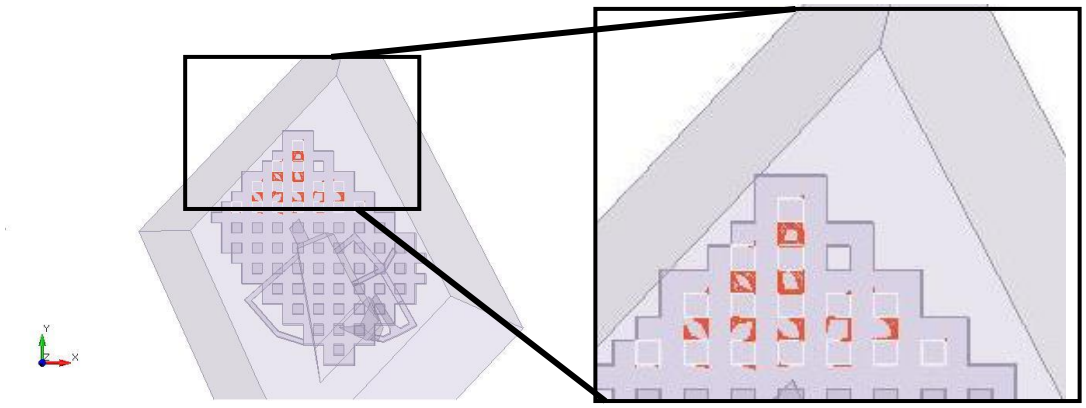

Figure 37. Stage three of the simulation were pillars are removed from the first area (BF2).

Moving on to the next stage, stage 4 or BF3, when rockfill pillars fill up the spaces created by the removal of the residual pillars are, it is when mostly all 0,9 strength factor isosurface disappears, having left only two spots where instabilities might happen. It is important to remember that, up to this stage, only the first area (the northest area), has suffered with backfill and pillar removal and that as seen in *Figure 32* left picture, excavation-length drifts are to be remained unbackfilled for them to allow mining operations.

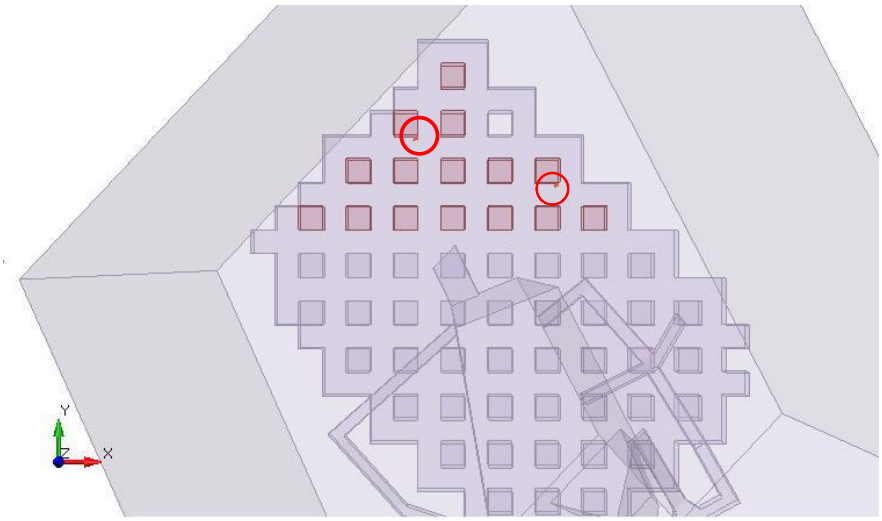

Figure 38. Backfill of the first area with some problematic areas left (BF3).

But as it can be seen in Figure 38, in stage 4 (BF3) where the second set of backfilled pillars are placed, the strength factor grows considerably and only two small spots are left with instability

issues. This phenomenon will occur along all the three areas and stages. It is important to notice that from stage 5 some stability problems will come in an area around the pit base contour.

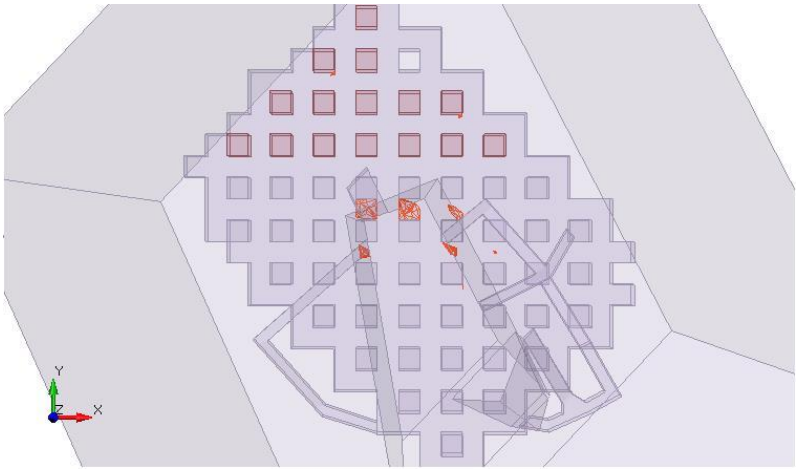

Figure 39. Problematic and potential instabilities in stage 5 (BF4).

These weaker areas will be such that not even with the second set of backfilled pillars it will be enough to ensure stability on the pit contour (Figure 39).

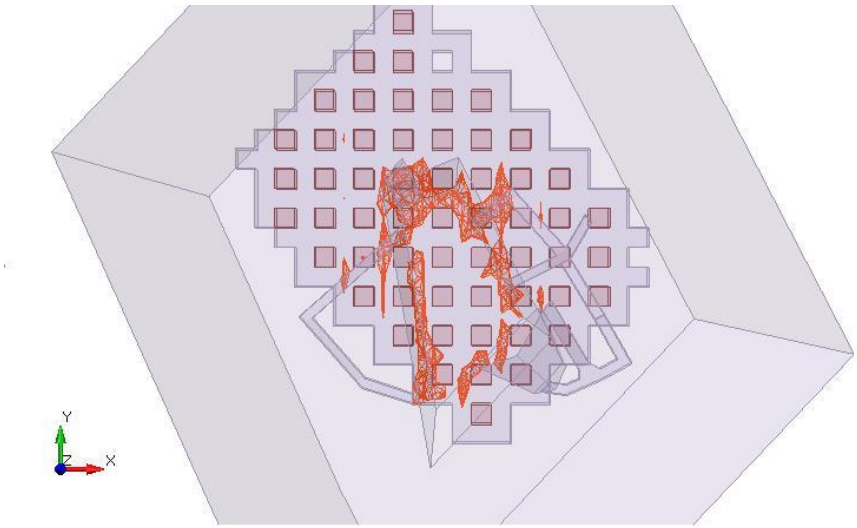

Figure 40.Final stage (BF9) of the excavation, all the area backfilled and a strength factor isosurface equal to 0,9.

Figure 40 shows a contour area around the open-pit limits that extends approximately 5 m around it, on the rockfilled pillars. This area increases in the north side of the open pit, indicating the influence of an already existing underground opening at level 156 m. It is important to notice that these instabilities will only occur in the rockfilled pillars and not on the floor and/or roof of the excavated volume or in any other part of the pit or surface.

For comparison reasons, a non-problematic area was analyzed as well, this means, a pillar out of the pit contour zone. This point was selected in a way that in any stage its strength factor was below 1,2. Randomly, the residual pillar 8_228 (Figure 41)(as named in the simulation) was studied.

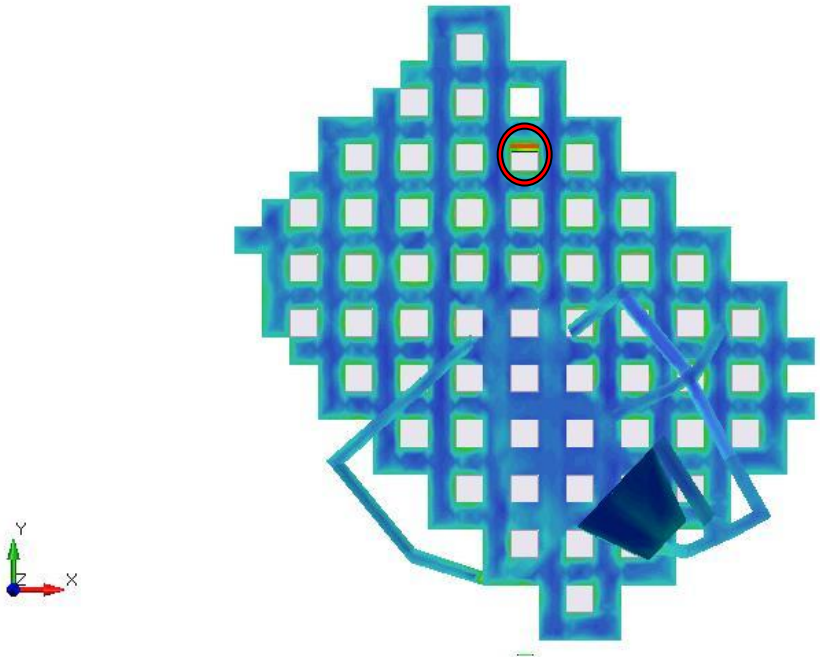

Figure 41. Visual representation of the localization of the residual pillar 8_228.

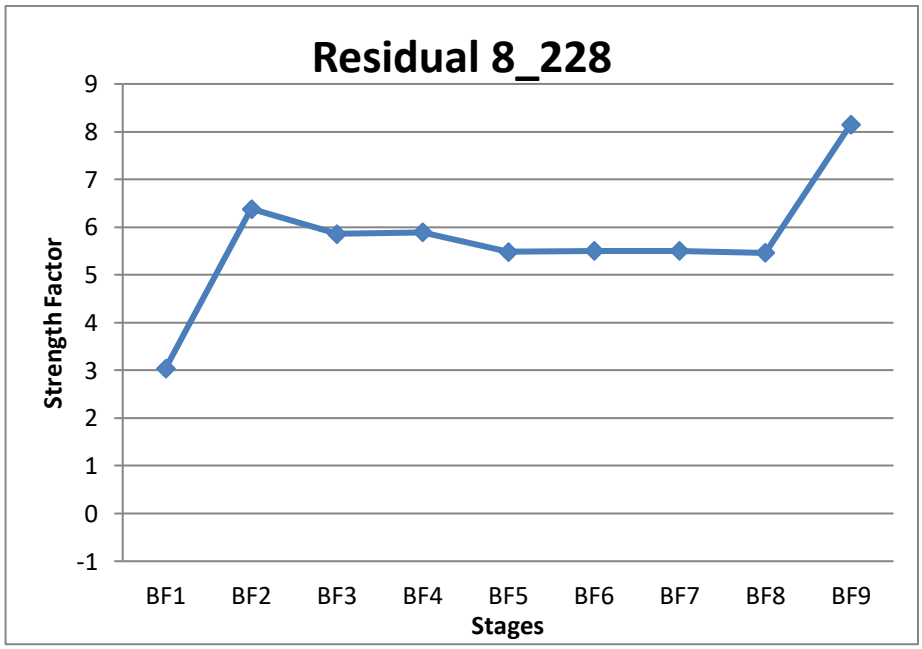

Figure 42. Strength factor variation with every stage of the simulation.

As it shows the aforementioned graph, Figure 42, for this pillar situated rather north in the excavation, the value of the strength factor initiates with an optimal value of approximately 3. In phase two it suffers an increase of this value most probably due to the rockfill of the immediate volume facing it. Through the stages it is shown no variation worth mentioning until, in the last stage, it goes under yet another increase of its value, possibly explained due to the total backfill of the excavation including the excavation-length drifts that were left empty to continue operations until last stage.

To summarize, for this particular case, the strength factor was increased with the rockfill phases.

5.2. State of stress

After the excavation and the following stages of backfilling, some induced tensions will occur. These induced tensions are those that are generated as a consequence of the modification of the state of natural stresses due to a tension readjustment around the excavations. When an underground excavation is carried out in a rock mass subjected to a previous stress state, the original stresses are redistributed around the created hole. The new principal stresses are perpendicular to each other but will be rotated with respect to the directions of application of the previous stresses.

The results can be systematized under two representations of the stress distribution in the modeled excavation, namely the distribution of average stresses (p) [26] and shear stresses ($\sigma_{i,j}$) [27], defined as follows:

$$p = \frac{\sigma_1+\sigma_3}{2} \quad [26]$$

and

$$\sigma_{i,j} = \frac{\sigma_1-\sigma_3}{2} \quad [27]$$

In the previous equations σ_1 and σ_3 represent the maximum and minimum principal stress, respectively. Thus, the distribution of normal stresses will provide important information in terms of failure planes and concentrated tensions while with the distribution shear stresses, as the name implies, concentration of tensions of this type. In this study effective stresses will be considered. For the main principal stress, the highest value found, for all stages, was 18,83 MPa and the lowest -0,41 MPa.

5.3. Correlation between the stress state and the strength factor

For the stress state analysis, points in the excavation were selected in order to assess the stress state as the staging advances. The study of induced stresses will be commented in correlation with the strength factor, to determine, which ones are the tensions that cause the strength factor to be so low. Following this premise, a point in the stage BF4 (stage 5) where pillars have not been removed yet, but rockfill pillars have been filled in order to support the empty volume that will happen on the next stage (BF5) (Figure 43), when residual pillar are removed, was selected due to its low strength factor and the instability tendency that shows around the pit contour. A RS3 tool called ‘query line’ allows value shading along a line in order to obtain detailed information where it was placed (Figure 44). In the next picture the query line can be seen where the strength factor was lower. Red and white cubes mean that these volumes are backfilled. Light gray cubes represent residual pillar, not

removed yet. This election is also corroborated with the plot of the strength factor in this line against the distance from the begging of the line, the northest point to the southest point, as seen in Figure 45, for being extremely low (-8,93).

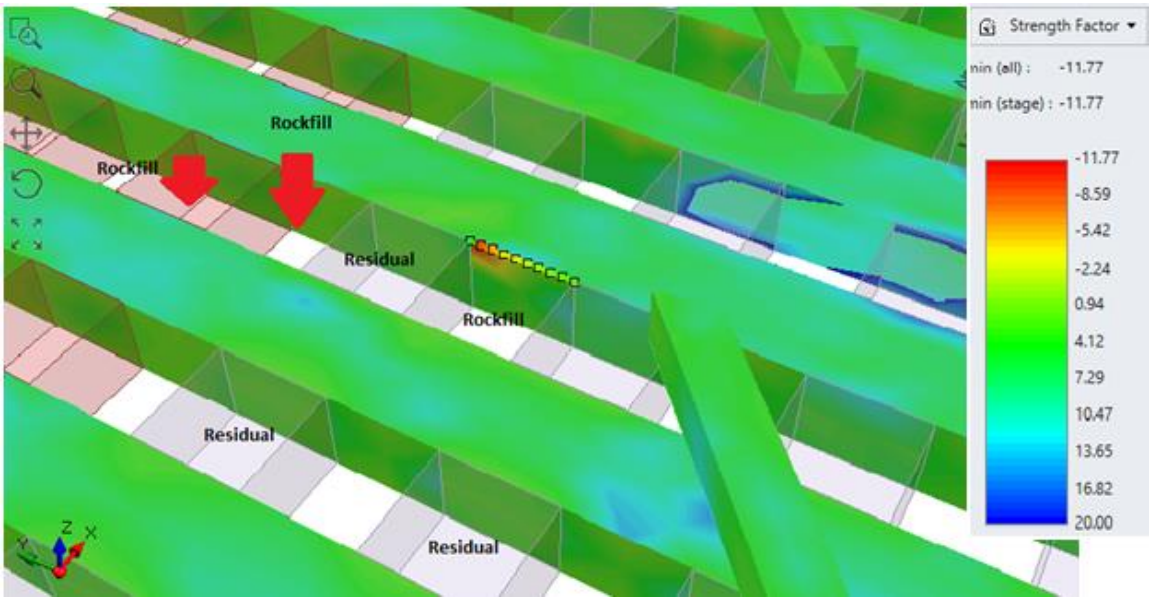

Figure 43. Position of query line along the top of a rockfilled pillar.

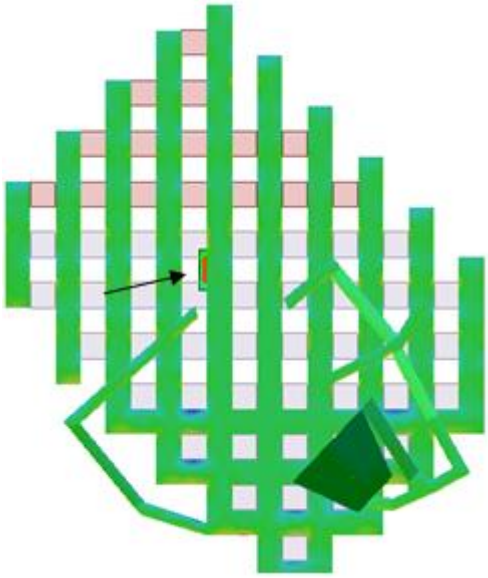

Figure 44. Position of query line in the top view of the excavation.

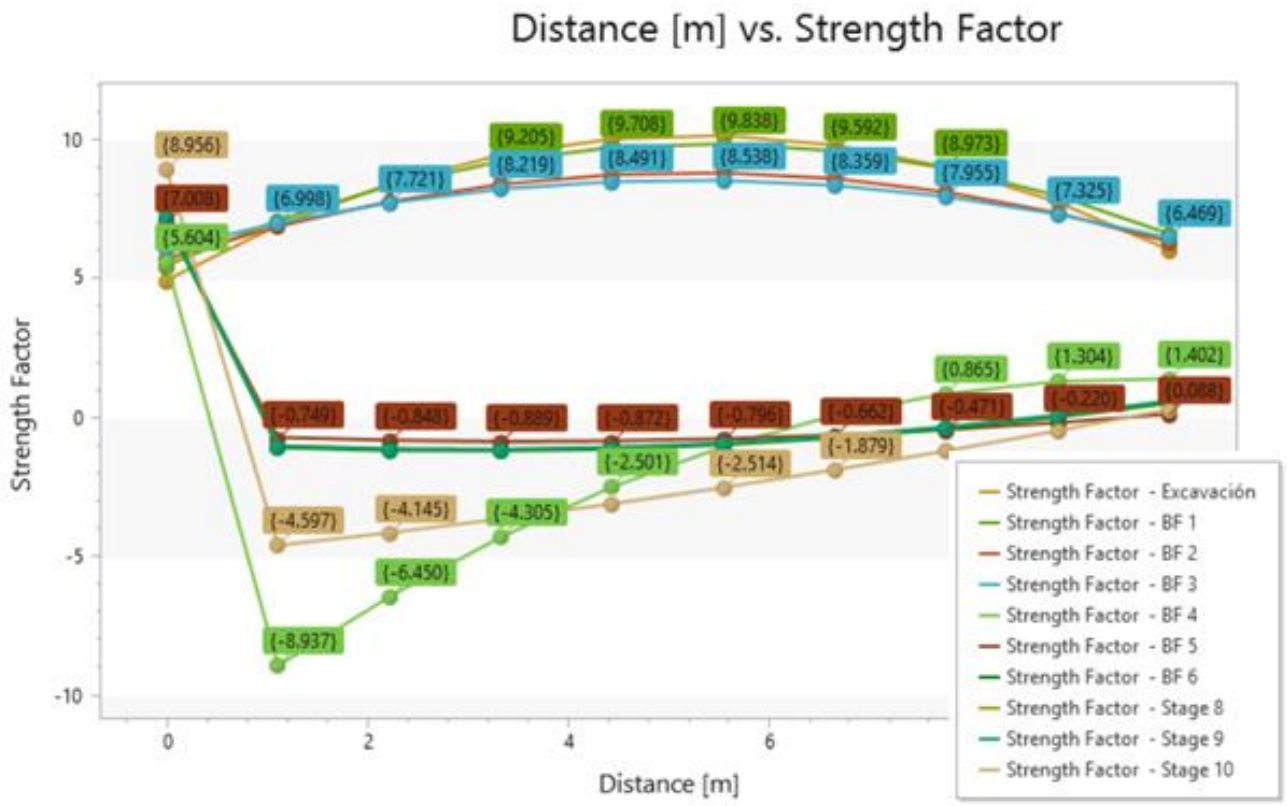

Figure 45. Strength factor plotted against each point at the query line.

So in order to determine which ones are the stresses that will create most of the instability, its graphical representation along the query line are presented (*Figure 45*), being inversely proportional the type of relation, i.e., the lower the strength factor is, the higher the stress around each point of the query line is. As commented in the previous title, information about the stress state will be given by the mean stress and the shear stress.

The explanation on the negative values for the strength factor comes from the definition of the strength factor itself. As stated before, the strength factor is the division the rock strength by the induced stress at every point in the mesh. This indicates that in such point were the strength factor is negative, some overstressing will happen.

Shear stress components

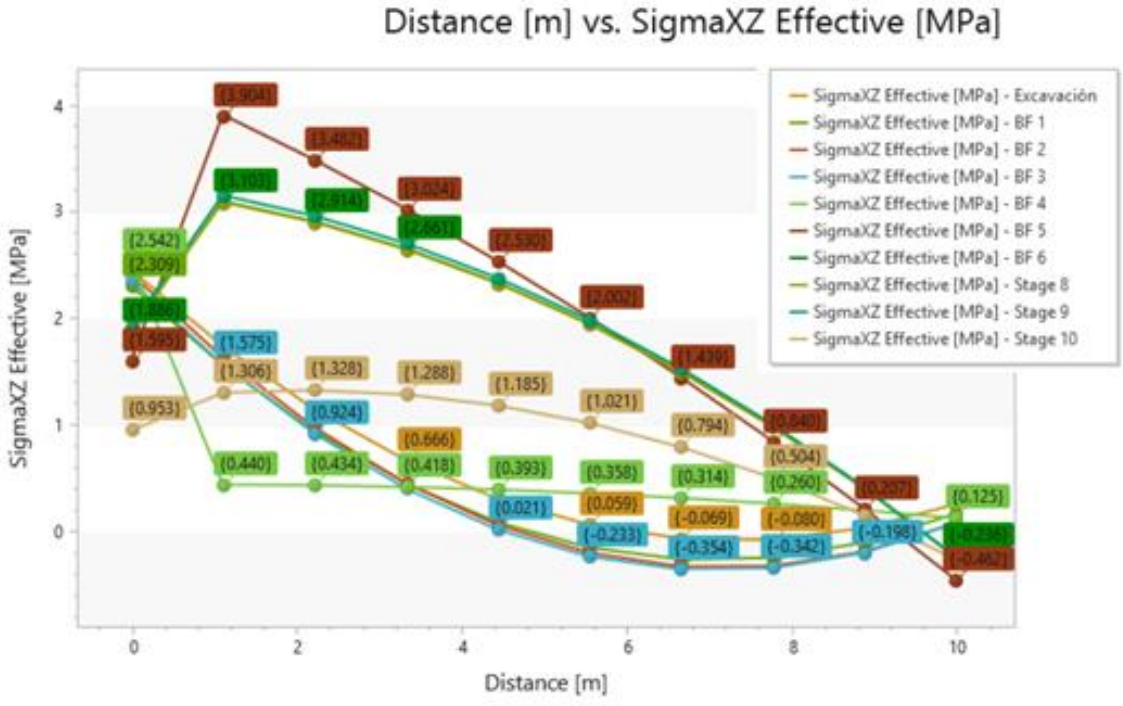

Figure 46. Distance against shear stress component XZ plot.

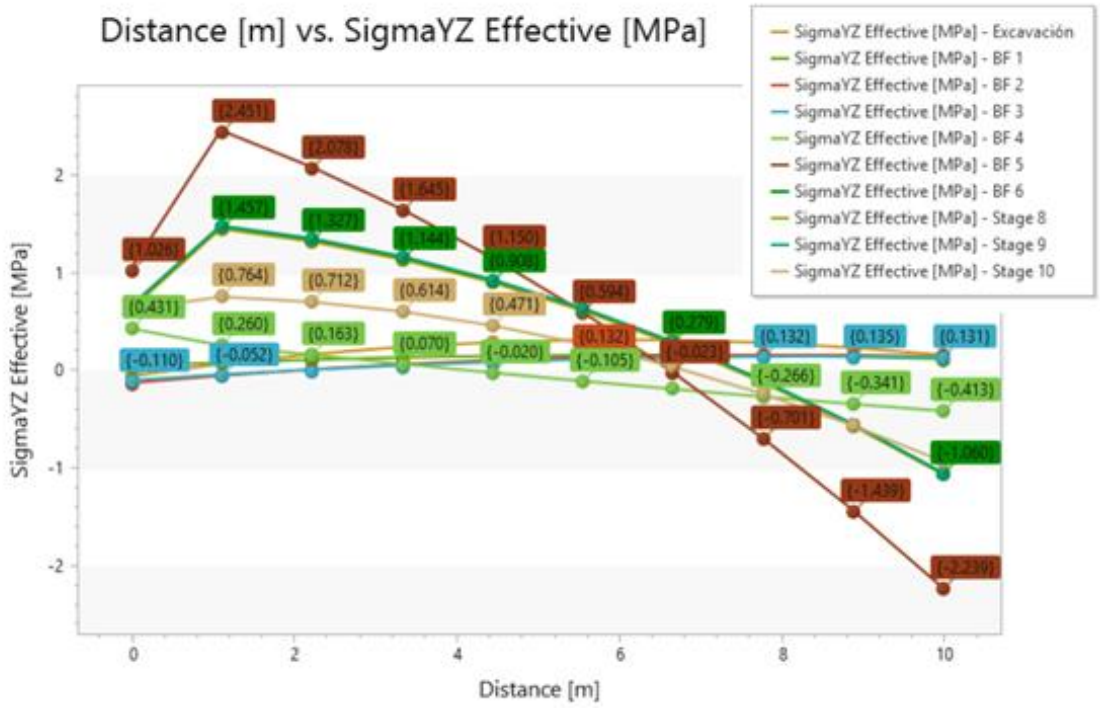

Figure 47. Distance against shear stress component YZ plot.

The shear stress values are higher for the stage BF5, which corresponds with the removal of the residual pillars and the solely support of the first shift of backfill pillars, which it would be expected. From looking at both graphs, shear stress on the plane XZ (*Figure 46*) will be higher than that in the plane YZ (*Figure 47*) (3,9 versus 2,45 MPa).

Mean stress

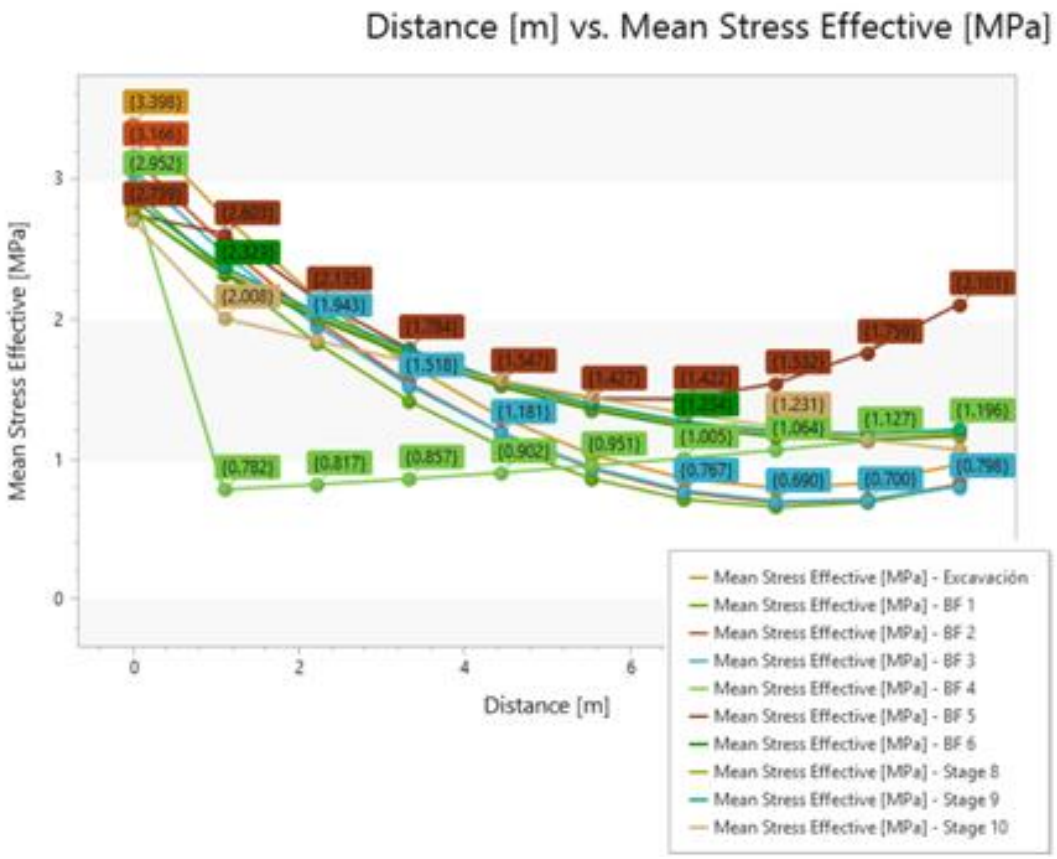

Figure 48. Distance against mean stress plot.

From the mean stress values, little correlation with the strength factor function can be deducted. Just a general observation that principal stresses did not vary substantially over time (*Figure 48*).

In general, from these graphs and the slopes of each function along the stages, it can be deducted that the shear stress on the plane XZ, is the main tension in the stress state that will cause the instability. It is also the one that shows the highest correlation on the temperature map.

Values on principal stresses, σ_1 and σ_3 are plotted in the chapter Annex.

5.3.1. Shear stress

For further analysis, the renderized contour plane option on RS3 to visualize shear stress components was used. As a 3D model, shear stress is represented both with τ_{xz} and τ_{yz} as z is the vertical axis that is parallel to the gravitational forces. From the strength factor chapter it can be first interpreted that there is an area were tensions accumulate and that is the immediate surroundings of the pit in the excavation.

As it can be seen in Figure 49, from stage 5 (BF 4) shear stress accumulate in the corners of the pit just above the excavation. This can be explained as principal stresses are very high in this area and

shear stress from the plane of the slope of the pit and the planes from the pillars are in opposite directions and this resulting in the location of intersection having the highest values of shear stress. This effect will be translated for the immediate pillars that set aside from the pit area. For this stage, shear stress goes from -5,04 MPa to 6,74 MPa.

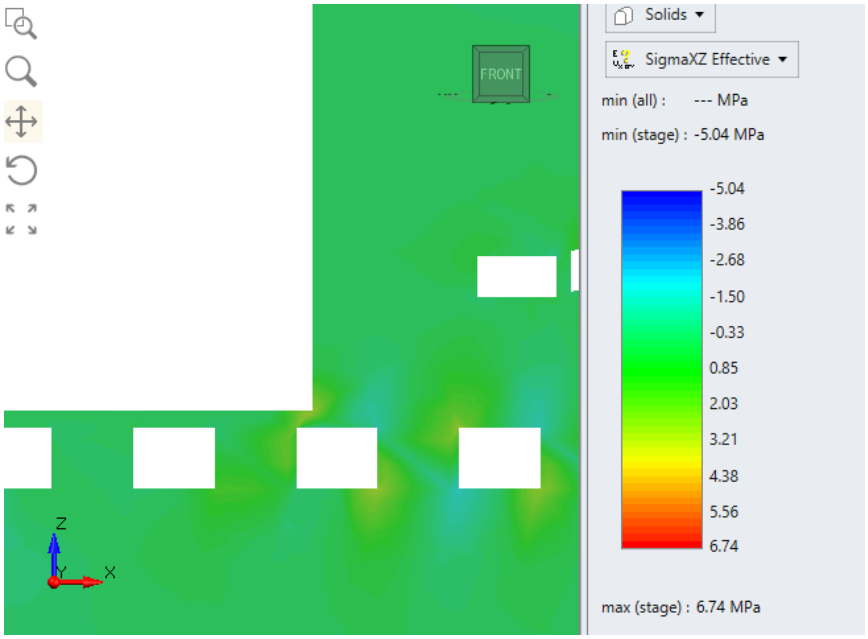

Figure 49 Shear stress XZ component on BF 4 profile.

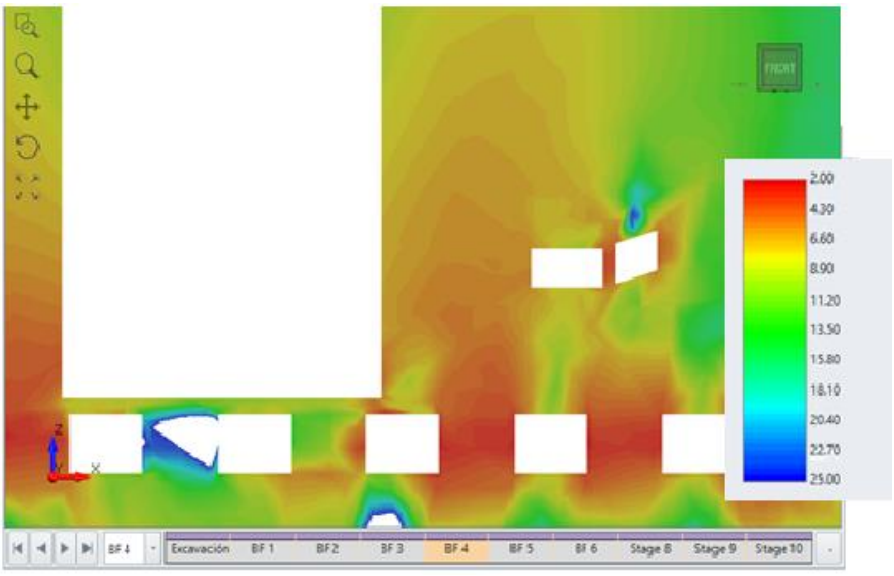

Figure 50. Strength factor for BF4 profile.

In the picture above, Figure 50, the same profile as in Figure 49 is presented but this time showing values for the strength factor. From the temperature map it can be see that lower values for the strength factor, correspond with the concentration of shears stress. For this stage and vertical cut, there is a minimum value of 2 and a maximum value of 25. Such high values belong to areas not excavated but still inside of the model scope.

Having this in mind, one last observation will be pointed is that in the last stage, even with every drift backfilled, the area will still suffer instabilities as it can be seen in the picture below (*Figure 51*), where the 0,9 isosurfaces appear in the backfilled area where the pit is.

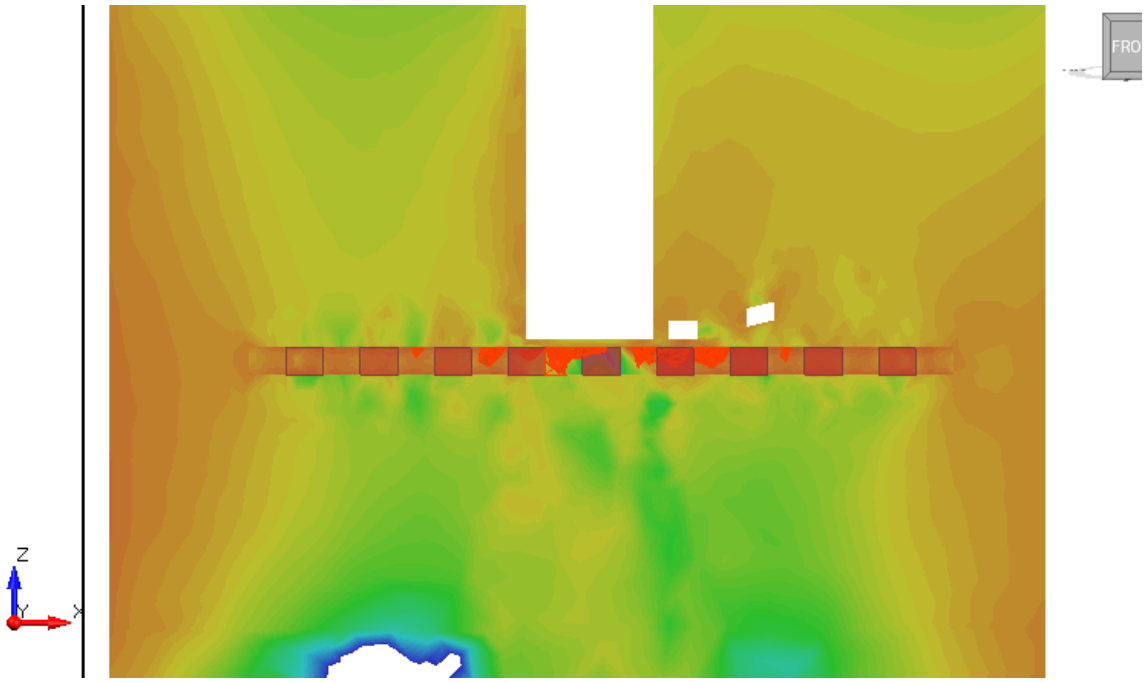

Figure 51. Strength factor on plane XZ with 0,9 strength factor isosurfaces (in red).

From the last picture, Figure 48, the 0,9 isosurface representation is shown along the excavation that, already in this final stage (BF9), has been backfilled. It is also important to note that lower strength factor values are represented mostly on the rockfill and not on the roof and/or floor of the excavation. This concludes that even though there exist values from the strength factor that are below 1, these are solely from the rockfill and not the rockmass.

5.4. Displacements

Finally, total displacements are analyzed in order to measure the impact of the room and pillar excavation in the existing pit, this is, slopes and surface foundation. From a contour plane, in the last stage, the highest affected due to the total backfill of the area, values from total displacements can be seen. After creating temperature vertical cut planes along the model it was observed that in a plane created along the sixth row, counting from the north, it was identified higher displacements.

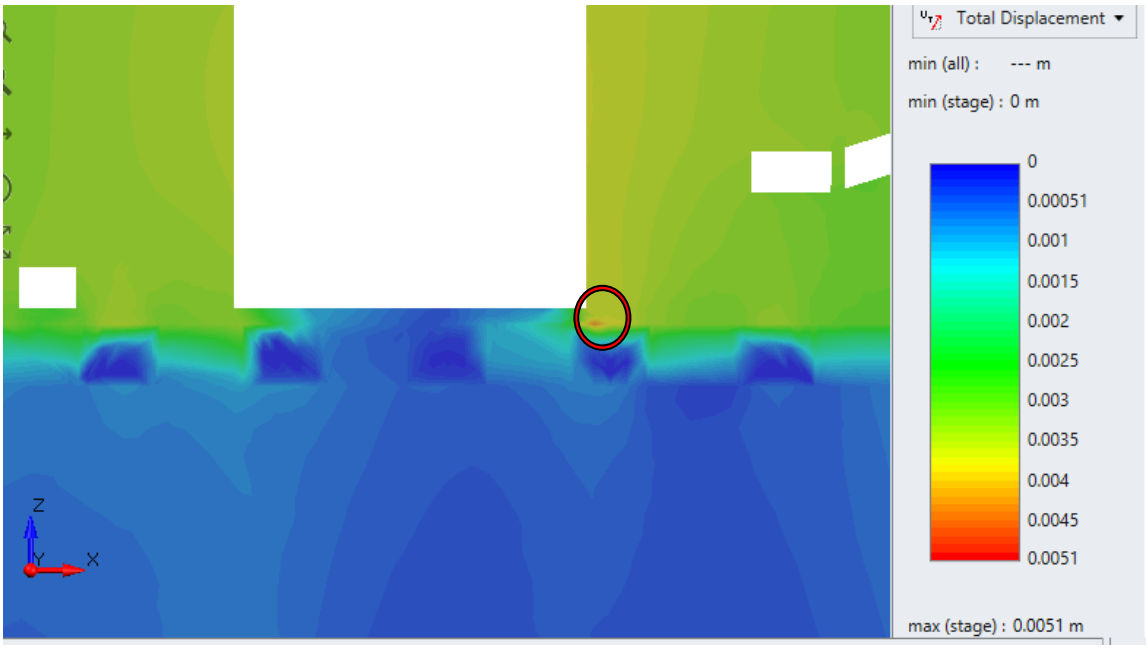

Figure 52. Temperature map on total displacements in stage BF9.

As it can be seen in Figure 52, there is an area near the left corner of the pit, where displacement reaches its highest value. Despite of this, this value is approximately 0,0051 m (which corresponds to a safety factor of 8) and represents little concern for global or local stability.

6. Conclusions and Further works

In this chapter some conclusions are going to be commended for every division of this thesis, this is, from the literature review, from the case study to the laboratory and field works that lead to the geomechanical characterization and finally from the methodology and the results. As a final act of this project, some recommendations will be done in order to establish a study line for this particular case.

From the literature review it can be deducted that there is plenty of information, scientific research and methodologies in the area of underground excavation and geotechnical analysis. These underground excavation overviews and studies, and specifically, in the room and pillar method, are most typically done for real cases for real mines and, in general, for coal or metallic deposits. It makes sense as these are the types of exploitations where underground mining methods are commonly applied. What came as less usual or less frequent is the utilization of the room and pillar mining method for underground quarries. Quarries are typically exploited via open pit methods, but some decades ago, when technology was advanced enough, the type of exploitation shifted, especially for lifelong quarries that open-cut operations were no longer feasible due to economical issues but particularly to environmental policies. Several scientific papers about underground quarries came out trying to find a common ground for this type of exploitation, especially from countries where natural stone production is quite high. Portugal is one of these top countries,

particularly in marble production. From the quarries in the area of Alentejo, in the last years, a small number of scientific articles, thesis and reports were done in the field of underground quarrying and it can be concluded that the present thesis is an insightful contribution to the geomechanical characterization of the region for new ways of quarrying.

With this project it was also intended to contribute to the present European policies on circular economy, by giving an alternative purpose to the waste material and at the same time recovering exploitable material increasing the benefits. These policies affect especially on the mining sector, where environmental laws have strictly dictated technical and financial feasibility. For this, it was suggested a way to follow this new pattern of business where residual material or tailings from the exploitation, accumulated in waste lands, was given a purpose not to only become a more environmentally-sound quarry but also a mean to improve mining recovery and act as an added support for the excavation. From this particular case, where an underground room and pillar excavation for marble was introduced to a backfill scenario, making use of the quarry's tailings, little information was proven to be found and, from that, it can be concluded that this paper, is, to say the least, innovative in this field of work.

From the case study, where all the laboratory tests were done, it is worth mentioning that the Borba-Estremoz-Vila Viçosa anticline is a unique scenario and a very competent marble deposit, in Portugal and in the world that has provided for the region over centuries. The laboratory works were the starting point for the modeling of the quarry and results were very consistent throughout the whole sample field, which made the material assignment process very straightforward.

The Finite Element Method and Finite Element Method Analysis were the proposed methodology for this subject and throughout all the process it was proven to be a very distinctive and smart solution to estimate and simulate engineering situations. An unmatched experience improved by the software used, RS3 from Rocscience Inc.

To be continued, some conclusions were draw from the chapter of results interpretation.

The importance of the state of stress in order to determine local and global stability for the proposed excavation is key to this study. After presenting the results in the chapter above some conclusions can be draw:

1. It seems to exist an area following the pit's contour, regarding the strength factor as a mean of determining stability, will not perform as expected and will inevitable cause failure on the rockfilled pillars. For this reason is recommendable that if ever exploited this area should be looked carefully. Thus, further analysis must be performed in order to determine a suitable method to avoid any kind of local instabilities or, as a last resource, by leaving the remaining rock pillars.
2. It can be concluded that the main component in the stress state, main source of lower strength factor, is the shear stress in the plane XZ. As it is expected due to pillars with low strength factor will lead to failure because of reaching the value of shear strength. It is also

important to mention that failure will be exclusively done on the rockfill volume and in no way it appeared that the floor or the roof of the excavation will cause rock fall or failure.

3. Displacements will occur as a local event, in the area where the shear stress is concentrated; this is, in the bottom corner of the pit. It is important to mention that these displacements are milimetric and present little to no impact on the quarry stability, neither on the slopes of it, nor in the surface. The obtained strength factor for these local events have a minimum of 8.
4. As it can be seen on the sequential removal of the pillars, instabilities appear when removing all residual pillars at once from one area. To ensure stability it is recommended that the removal of these marble pillars and the following backfill is done individually for each volume, i.e. when a pillar is removed, before removing the others from the same area, backfill immediately and so on. It is also recommended a further analysis on backfilling and remaining pillar extraction sequence to better understand the instability process and look for alternatives.
5. Finally, to point out that out of the problematic area, as presented in Figure 39, most of the excavation will demonstrate a positive effect of the rockfill support as an increase of the strength factor will happen, on the rockfilled pillars, as stages advance, up to the last stage, with the total backfill of the excavated area, that the strength factor will increase even higher.

To finalize, a series of further works are stated to motivate future researchers on this line of study.

It is critical to continue the investigation on research projects for the area of the Alentejo in Portugal as it unique condition makes the area a great scenario to improve the state in terms of benefits for the region, and overall, to Portugal. It is also worth mentioning that if the line of the sequenced rockfill excavation is carried out, it is imperative to make follow ups on the local stability and the backfill and removal operations, recommending carrying them out individually for each pillar, as explained on the list above.

7. Bibliography

Almeida, J., & Nunes Costa, C. (2000). *Análise Geomecânica Da Exploração Subterrânea Da Pedreira " Texugo ." 31*(May 2006).

Alonso, E., Gens, A., & Josa, A. (1990). Constitutive Model for Partially Saturated Soils. *Géotechnique*, *40*. https://doi.org/10.1680/geot.1990.40.3.405.

Bloss, M. L. (2014). An operational perspective of mine backfill. In Y. Potvin, Y. Potvin, T. Grice, & T. Grice (Eds.), *Eleventh International Symposium on Mining with Backfill* (pp. 15–30). Australian Centre for Geomechanics PP - Perth.

Brady, B. H. G., & Brown, E. T. (2006). Rock Mechanics for underground mining. *Springer*, *January 2006*.

Brown, E. T., & Hoek, E. (1980). *Underground excavations in rock* (E&FN Spon (ed.); https://es.scribd.com/doc/56764887/Hoek-Brown-Underground-Excavation-in-Rock.

Bunting, D. (1911). Chamber pillars in deep anthracite mines. *Trans AIME*, *42*, 236–245.

Campo, M. E. A. del, Naranjo, F. J. F., González, J. C. A., Gómez, V. R., Angeles Perucha, M., Estévez, L. V., de la Losa Román, Almudena , Estévez, C. B., & Pacheco Rodríguez, R. (2018). *Guía para la rehabilitacion de huecos mineros con residuos de construcción y demolición (RCD)*.

Carvalho, J. F., Henriques, P., Falé, P., & Luís, G. (2008). Decision criteria for the exploration of ornamental-stone deposits: Application to the marbles of the Portuguese Estremoz Anticline. *International Journal of Rock Mechanics and Mining Sciences*, *45*(8), 1306–1319. https://doi.org/https://doi.org/10.1016/j.ijrmms.2008.01.005.

Carvalho, J., Filipe, A., Inverno, C. M. C., Oliveira, D. P. S. de, Santana, H., Matos, J. X. de, Ramos, J. F., Batista, M. J., Sardinha, R., Salgueiro, R., Lisboa, V., Leite, M., Moura, C., Martins, L., & Costa, L. (2010). Recursos minerais: o potencial de Portugal. *LNEG, Laboratório Nacional de Energia e Geologia*, 1–74.

Carvalho, J. M. F., Carvalho, C. I., Lisboa, J. V, Moura, A. C., & Leite, M. M. (2013). Portuguese ornamental stones. *Geonovas*, 15–22.

CERENA. (2019). *Estudo da estabilidade das escavações subterrâneas na pedreira Monte d'el Rei MJ - 5282*. Relatório técnico não publicado.

CERENA. (2020). *Estudo da estabilidade das escavações subterrâneas na pedreira Monte d'el Rei MJ - 5282*. Relatório técnico não publicado.

Correa Arroyave, Á. (1991). Galerías mineras: la modelización analítica como una ayuda geomecánica para el diseño minero. *Ingeniería e Investigación*, *25*, 10–19.

Costa e Silva, M. M. (2002). *Zonamento Das Propriedades Geotécnicas Dos Mármores Portugueses.* 8th Congresso Nacional de Geotecnia, Lisboa.

Courant, R. (1943). Variational methods for the solution of problems of equilibrium and vibration. *Bulletin of the American Mathematial Society*, *49*, 1–23.

de Araujo, F. C., & Pereira, R. A. T. (2017). Boundary-integral-based process for calculating stiffness matrices of space frame elements with axially varying cross section. *Engineering Analysis with Boundary Elements*, *77*, 61–69. https://doi.org/https://doi.org/10.1016/j.enganabound.2017.01.005.

Direção Geral de Energia e Geologia - DGEG. (2016). *Guião De Pedreiras*. https://www.dgeg.gov.pt/media/wzrozybv/gui%C3%A3o-.

Duvall, W. I. (1976). General Principles Of Underground Opening Design In Competent Rock. In *The 17th U.S. Symposium on Rock Mechanics (USRMS)* (p. 12). American Rock Mechanics Association.

Esterhuizen, E., Dolinar, D., & Ellenberger, J. (2010). Roof span design for underground stone mines. *Proceedings - 29th International Conference on Ground Control in Mining, ICGCM*, 318–324.

Esterhuizen, G S, Dolinar, D. R., & Ellenberger, J. L. (2008). Pillar strength and design methodology for stone mines. *Proceedings of the 27th International Conference on Ground Control in Mining. Morgantown WV: West Virginia University*, *9*, 241–253.

Esterhuizen, G S, Dolinar, D. R., & Ellenberger, J. L. (2011). Pillar strength in underground stone mines in the United States. *International Journal of Rock Mechanics and Mining Sciences*, *48*(1), 42–50. https://doi.org/10.1016/j.ijrmms.2010.06.003.

Esterhuizen, Gabriel S., Dolinar, D. R., & Ellenberger, J. L. (2011). Pillar and roof Span Design in Stone Mines. *Department Of Health And Human Services, NIOSH*, 75.

Federal Highway Administration. (2016). *User Guidelines for waste and byproduct materials in pavement construction*.

Ferrero, A. M., Migliazza, M., Segalini, A., & Gulli, D. (2013). In situ stress measurements interpretations in large underground marble quarry by 3D modeling. *International Journal of*

Rock Mechanics and Mining Sciences, *60*, 103–113. https://doi.org/10.1016/j.ijrmms.2012.12.008.

Focus Piedra. (2019, February 18). El tamaño del mercado mundial de mármol aumentará un 3,1% para 2025. *Periódico Digital de La Industria de La Piedra*, https://www.focuspiedra.com/el-tamano-del-mercado-.

González de Vallejo, L., Ferrer, M., Ortuño, L., & Oteo, C. (2002). Ingeniería Geológica. In *Editorial Pearson Education, Madrid*.

Haixiang, Z. (1999). Superficial views on tight-fill ratio of ascending drift-and-fill. *Mining and Metallurgy*.

Harish, A. (2020). *Finite Element Method - What is it? FEM and FEA explained*. SIMSCALE Blog. https://www.simscale.com/blog/2016/10/what-is-finite-element-method/.

Hedley, D. G. F., & Grant, F. (1972). *Stope-and-Pillar Design for the Elliot Lake Uranium Mines*. Canadian Institute of Mining, Metallurgy and Petroleum.

Herrera, J. (2007). *Diseño de Explotaciones de Cantera*. http://oa.upm.es/21839/.

ISRM. (1978). SM for Determining the Strength of Rock Materials in Triaxial Compression. In R. Ulusay & J. A. Hudson (Eds.), *The Complete ISRM Suggested Methods for Rock Characterization, Testing and Monitoring:1974-2006*.

ISRM. (1979). SM for Determining the Uniaxial Compressive Strength and Deformability of Rock Materials. *Int J Rock Mech Min Sci*, *16 (2)*, 135–140.

ISRM. (2006). *The Complete ISRM Suggested Methods for Rock Characterization, Testing and Monitoring:1974-2006* (R. Ulusay & J. A. Hudson (eds.)).

Kim, J.-G., Mohamed Ali, M., & Yang, H.-S. (2018). Robust Design of Pillar Arrangement for Safe Room-and-Pillar Mining Method. *Geotechnical and Geological Engineering*. https://doi.org/10.1007/s10706-018-0734-1.

Kojo, I. V, Reuter, M. A., & Heiskanen, K. (2013). Some examples of reuse , repurposing and recycling of minerals to improve the resource efficiency in mining. *6th International Conference on Sustainable Development in the Minerals Industry, 30 June – 3 July 2013, Milos Island, Greece*, *July*, 386–389.

Kosmatka, S., Kerkhoff, B., & Panarese, W. (2002). *Design and Control of Concrete Mixtures*. Portland Cement Asociation.

Lèbre, É., Corder, G., & Golev, A. (2017). The Role of the Mining Industry in a Circular Economy: A

Framework for Resource Management at the Mine Site Level. *Journal of Industrial Ecology*, *21*(3), 662–672. https://doi.org/doi:10.1111/jiec.12596.

LNEG. (2007). *Mármores e calcários ornamentais de Portugal*. https://www.lneg.pt/wp-content/uploads/2020/05/Livro_Marmores_e_Calcarios_2007.pdf.

Lopes, L. (2007). O triângulo do mármore: estudo geológico. *Monumentos: Revista Semestral de Edifícios e Monumentos*, *27*, 158.

Lopes, L., Pinho, A., Duarte, I., & Martins, R. (2019). Caracterização e avaliação de riscos geológios e geotécnicos na pedreira nº 5282 Monte d'El Rei MJ. In *Journal of Chemical Information and Modeling* (Vol. 53, Issue 9). https://doi.org/10.1017/CBO9781107415324.004

Lunder, P. J., & Pakalnis, R. C. (1997). Determination of the strength of hard-rock mine pillars. *CIM Bulletin*, *90*, 51–55.

Martinez, A. F. (n.d.). *Sesión 1 Una introducción de Análisis Numérico para aplicaciones Geotécnicas Objetivos de Aprendizaje*.

Muralha, J., Grasselli, G., Tatone, B., Blumel, M., Chryssanthakis, P., & Jiang, Y. (2014). ISRM Suggested Method for Laboratory Determination of the Shear Strength of Rock Joints: Revised Version. *Rock Mechanics and Rock Engineering*, *47*, 291–302. https://doi.org/10.1007/s00603-013-0519-z.

Murch, A. (2018). *Dimensionamento de Bancadas Ascendentes Engenharia Geológica e de Minas*. Instituto Superior Técnico - Universidade de Lisboa. https://fenix.tecnico.ulisboa.pt/downloadFile/1970719973967874/Tese-AlexanderMurch.pdf.

Neville, A. M. (2009). *Properties of concrete* (Pearson Education Limited (ed.); 5th ed.). Prentice H.

Oggeri, C., M.Fornaro, Oreste, P., & D.Valentino. (2001). *Going Underground in Quarrying: Technical Perspectives for Marble in Portugal*.

Oggeri, C., & Oreste, P. (2015). Underground Quarrying for Marble: Stability Assessment through Modelling and Monitoring. *International Journal of Mining Sciences (IJMS)*, *1*(1), 35–42.

Oldecop, L. A., & Alonso, E. E. (2013). Rockfill mechanics. *Advances in Unsaturated Soils - Proceedings of the 1st Pan-American Conference on Unsaturated Soils, PanAmUNSAT 2013*, 61–86. https://doi.org/10.1201/b14393-7.

OpenLearn. (n.d.). *Introduction to finite element analysis*. Retrieved July 26, 2020, from https://www.open.edu/openlearn/science-maths-technology/introduction-finite-element-analysis/content-section-0?active-tab=description-tab.

Palma Guerreiro, H. J. (2000). *Exploração subterrânea de mármores*. Instituto Superior Técnico - Universidade de Lisboa. http://www.visaconsultores.com/pdf/Tese_MSc_HG.pdf.

Paneiro, G. (2014). *Uso de Técnicas de emissão acústica e atividade microssísmica para apoio de projetos geotécnicos sobre maciços rochosos*. Dissertação para a obtenção do grau de Doutor em Georrecursos. I.S.T.

Rankine, R., Pacheco, M., & Sivakugan, N. (2007). Underground mining with backfills. *Soils and Rocks*, *30*(2), 93–101.

Roberts, D., Tolfree, D., & McIntire, H. (2007). Using Confinement As a Means to Estimate Pillar Strength In a Room And Pillar Mine. In *1st Canada - U.S. Rock Mechanics Symposium* (p. 7). American Rock Mechanics Association.

Rocscience Inc. (n.d.). *Strength Factor Data Contours in RS2 Interpret*. https://www.rocscience.com/help/rs2/phase2_interpret/Strength_Factor.htm#:~:text=Data %3E Strength Factor-,Strength Factor Data Contours in RS2 Interpret,every point in the mesh.

Rodrigues, J. J. P., Guerreiro, L. F. P., Salvador, A. J., & Oliveira, L. M. (1993). Backfill Practices At the Neves Corvo Mine, Portugal. In *ISRM International Symposium - EUROCK 93* (p. 9). International Society for Rock Mechanics and Rock Engineering.

Salamon, M. D. G., & Munro, A. H. (1967). A study of the strength of coal pillars. *J S Afr Inst Min Metall*, *68*, 55–67.

Sarathchandran, A. (2014). Three dimensional numerical modelling of coal mine roadways under high horizontal stress fields. *University of Exeter*.

Sayas, F. J. (2008). *A gentle introduction to the Finite Element Method An introduction*. http://scholar.google.es/scholar_url?url=https://team-pancho.github.io/teaching/math838/anIntro2FEM_2015.pdf&hl=es&sa=X&scisig=AAGBfm0hKDqYdaoyqxh89qdVFzhLKSGJog&nossl=1&oi=scholarr.

Schleinig, J.-P., & Konietzky, H. (2017). *Geomechanical issues in room and pillar mining – an introduction*.

Shrestha, B. K., Tannant, D. D., Proskin, S., & Greer, J. R. & S. (2008). Properties of cemented rockfill used in an open pit mine. *GeoEdmonton'08*, 609–616.

Sivakugan, N., Veenstra, R., & Niroshan, N. (2015). Underground Mine Backfilling in Australia Using Paste Fills and Hydraulic Fills. *International Journal of Geosynthetics and Ground Engineering*, *1*. https://doi.org/10.1007/s40891-015-0020-8.

Süli, E. (2019). *Lecture Notes on Finite Element Methods for Partial Differential Equations*. *February*.

Talbot, A., & Richart, F. (1923). The strength of Concrete: Its relation to the cement aggregates and water. *Engineering Experiment Station*, *XXI*(7).

Tesarik, D. R., Seymour, J. B., & Yanske, T. R. (2009). Long-term stability of a backfilled room-and-pillar test section at the Buick Mine, Missouri, USA. *International Journal of Rock Mechanics and Mining Sciences*, *46*(7), 1182–1196. https://doi.org/10.1016/j.ijrmms.2008.11.010.

Tesarik, D. R., Seymour, J. B., Yanske, T. R., & Mckibbin, R. W. (1995). Stability analysis of a backfilled room-and-pillar mine. *Stability*.

US Bureau of Reclamation Engineering. (1977). Design Criteria for Concrete Arch and Gravity Dams. *Water Resources*, *19*.

Vintem, C., Lopes, L., Lamberto, V., Barros, R., & Costa, C. (1998). Mármores de Estremoz: Geologia, Prospecção, Exploração, Valorização e Ordenamento da Jazida. *Livro Guia Das Excursões. Instituto Geológico e Mineiro*, 191–200.

Warren, S. N., Raffaldi, M. J., Dehn, K. K., Seymour, J. B., Sandbak, L. A., Armstrong, J., & Ferster, M. (2018). Estimating the strength and mechanical properties of cemented rockfill for underhand cut-and-fill mines. *52nd U.S. Rock Mechanics/Geomechanics Symposium*, *June*.

Wu, J., Feng, M., Xu, J., Qiu, P., Wang, Y., & Han, G. (2018). Particle size distribution of cemented rockfill effects on strata stability in filling mining. *Minerals*, *8*(9). https://doi.org/10.3390/min8090407.

Zhou, N., Yan, H., Jiang, S., Sun, Q., & Ouyang, S. (2019). Stability analysis of surrounding rock in paste backfill recovery of residual room pillars. *Sustainability (Switzerland)*, *11*(2), 1–13. https://doi.org/10.3390/su11020478.

8. Annex

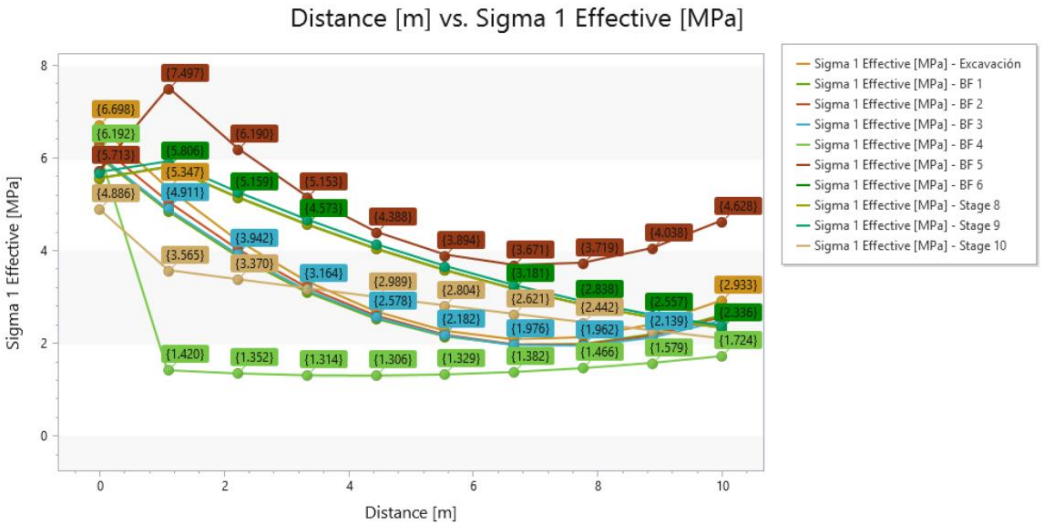

Figure 53. Sigma 1 (σ_1) plotted against all the points on the query line

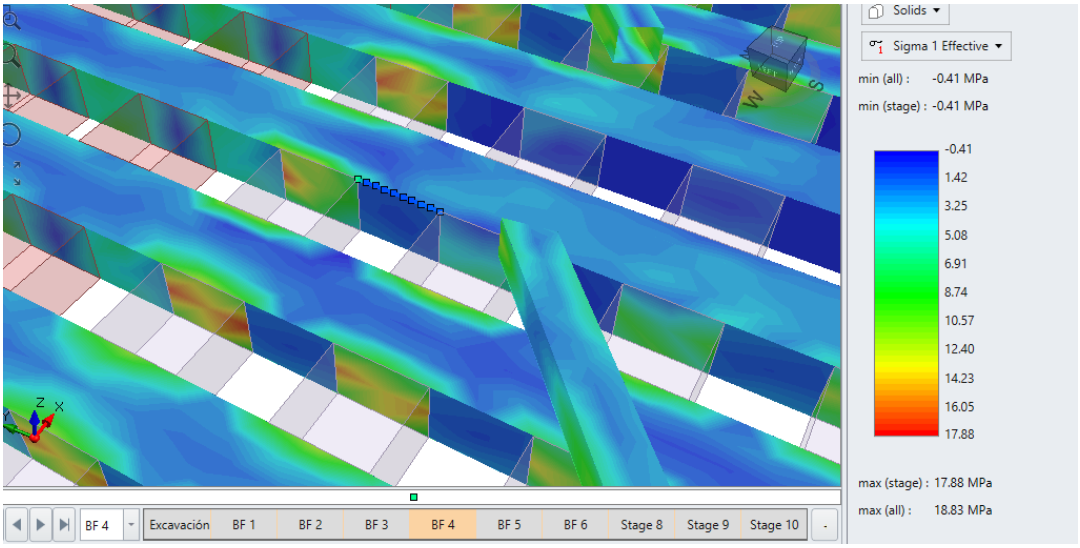

Figure 54. Temperature map on BF4 for sigma 1

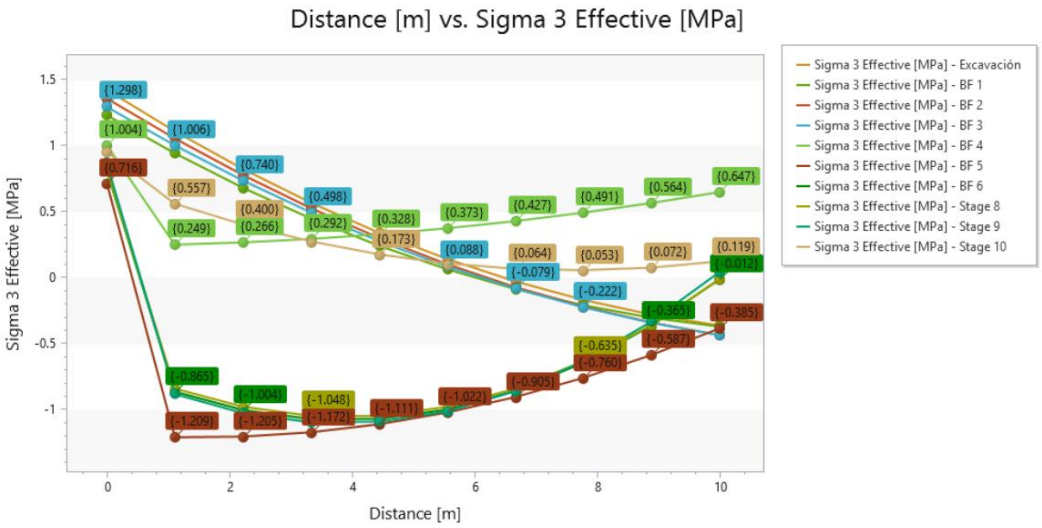

Figure 55. Sigma 3 (σ_3) plotted against every point in the query line